Characterization of the Spatio-Temoral Variability of the ABL Depths Observed During MATERHORN-X 1

S. Pal[1], S.F.J. De Wekker[1], G.D. Emmitt[2], K. Godwin[2], E. Pardyjak[4], L. Leo[3], S. Hoch[4], S. Sabatino[3], D. Zajic[5], M. Sghiatti[1] et al.

[1] University of Virginia. VA
[2] Simpson Weather Associates, VA
[3] University of Notre Dame, Notre Dame, IN
[4] University of Utah, Utah
[5] Dugway Proving Ground, Dugway, Utah

Aerosol stratification

Entrainment processes near the top of the ABL

Inversion with different strengths

Orographical Effect

Under different atmospheric conditions

Zi = Top of the ABL

MOUNTAIN TERRAIN ATMOSPHERIC MODELING AND OBSERVATIONS (MATERHORN)

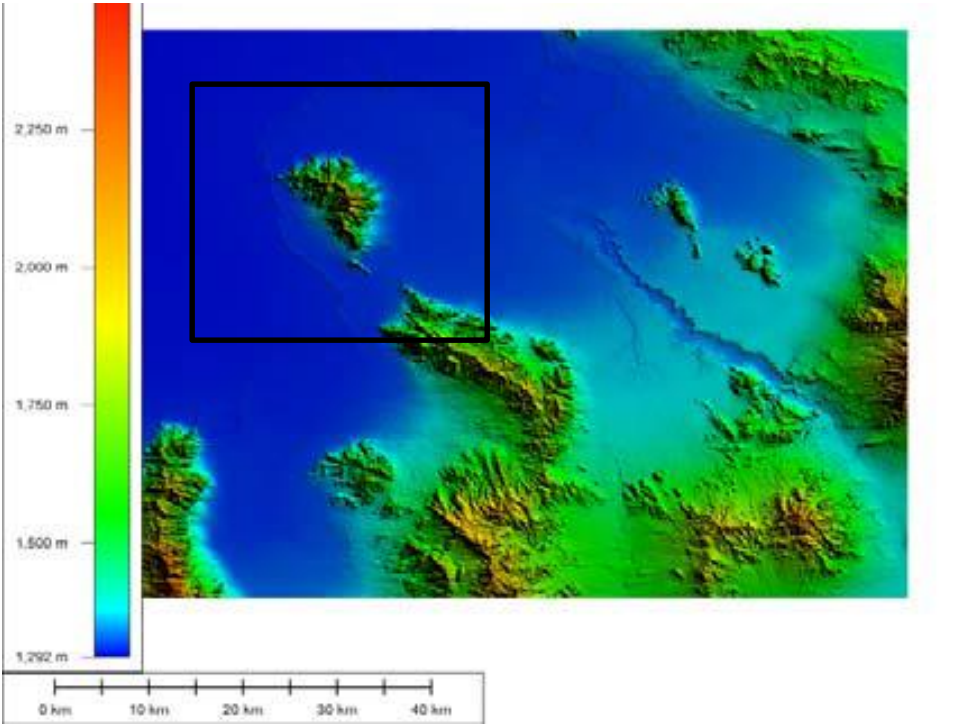

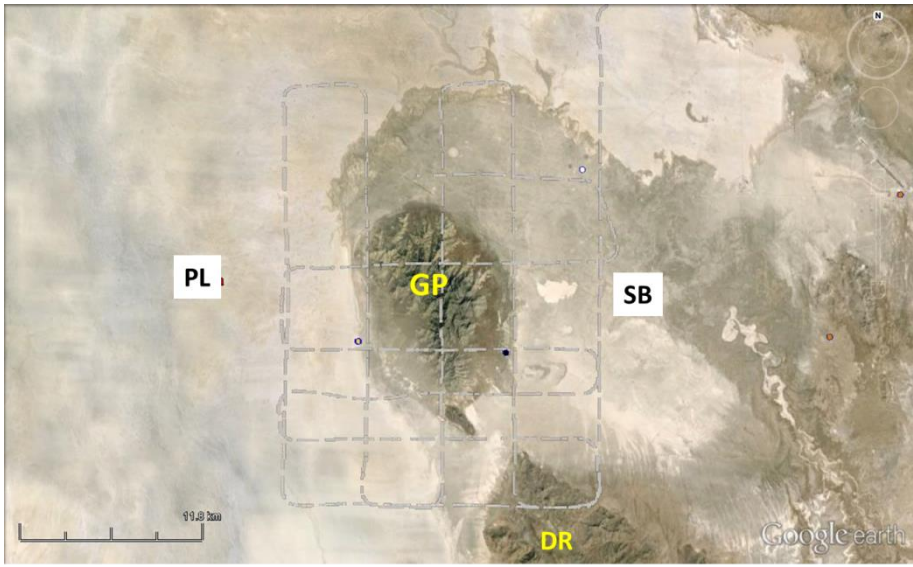

My research interests within MATERRHORN

- **Boundary layer depth variability over low-mountain area like DPG**
- Turbulence characterization combining ground-based and aircraft measurements
- Investigation of both morning and evening transitions in low mountain region

What's there in Today's Menu?

Investigation of CBL mixing and turbulence features

1. **Motivation** and background
2. Pre-MATERRHORN **findings** and general overview **(ABL-perspective)**
3. **Near-surface** meteorological conditions (standard PTU)
4. **Micro-me**t characterization (high resolution EC data at around Playa and SB)
5. **Thermodynamic** characteristics in the lower troposphere (RS-obs)
6. **Daily variability of** ABL depths (RS observations at two sites (thus general features in the **spatial-variability**)
7. **Spatial variability** in ABL depths and features observed in aerosol layers atop ABL (results obtained from TODWL measurements)
8. **Spatial variability in zi: underlying processes**

Motivation

- The height of the ABL, zi, is a fundamental variable of ABL
- Largest variability contrary to any other part of the earth's atmosphere; majority of the sources and sinks are located in the ABL
- Investigation of the spatio-temporal variability of zi in mountainous areas is urgent
- The turbulence parameterization of the CBL is an essential component of all weather and climate models which determines the quality of the simulation of wind, water-vapor, and temperature fields in the CBL.
- Correct estimation of CBL turbulence features and parameterization is a prerequisite for an accurate simulation of convection initiation as well as the development of clouds and precipitation
- A detailed understanding of spatial and temporal variability in zi is required for many meteorological applications

Particle pollution and gases are primarily trapped within the ABL.
Aerosols can be used as tracer of height and dynamics within ABL.

For a comprehensive investigation of atmospheric processes, lidar systems are highly beneficial because they provide volume data of atmospheric key parameters with high accuracy and resolution.

Spatial variability of daytime CBL height using airborne measurements

Applying Haar wavelet transform on the TODWL-derived high-resolution aerosol backscatter profiles, the spatial variability in z_i around the Granite Peak is investigated to:

1. determine the roles of both the complex topography and the changes in the surface forcing owing to the land-surface heteorogity on the spatial variability in z_i in a mesoscale domain.

2. characterize the ABL thermodynamic features and the z_i variability during the selected IOPs so that the MATERHORN community can use these information for myriad research purposes (e.g., scaling of turbulence features, CBL parameterization, idealized simulation, model evaluation as well as data assimilation)

Temporal evolution of CBL in innermost domain (66x66km)

WRF –DPG model results

OCTOBER 2200 UTC

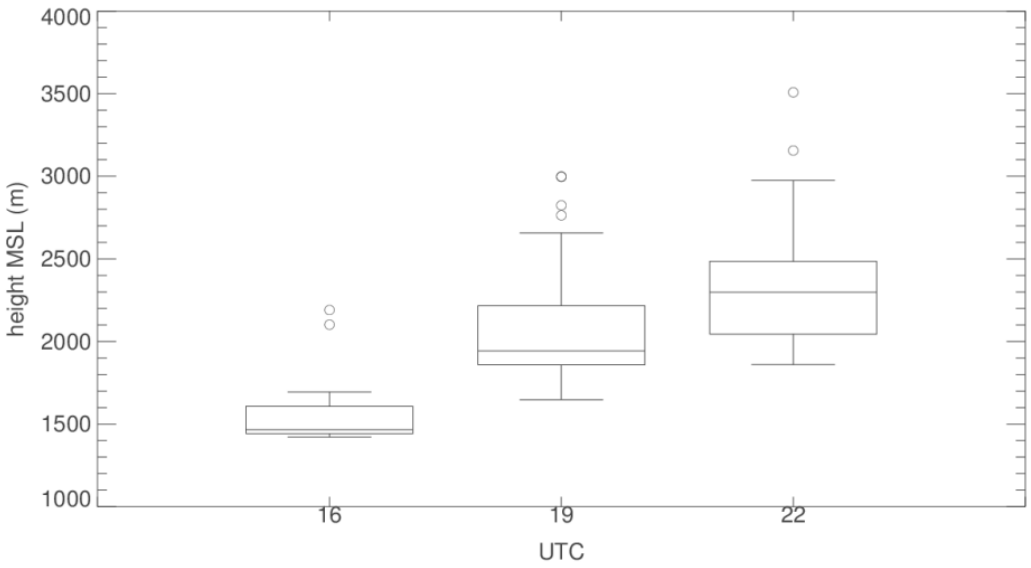

Spatial variability in CBL heights

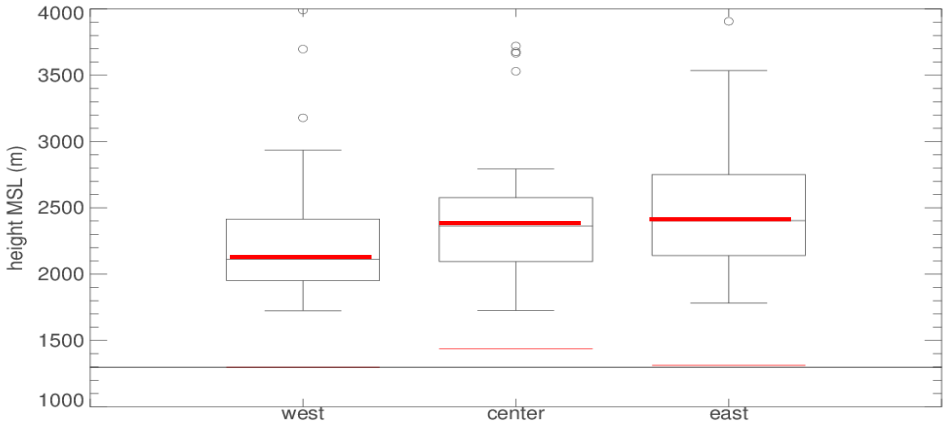

WEST CENTRAL EAST

Wavelet transform method to determine ABL depths

Haar Wavelet Transform method

Equation: 1

Haar wavelet is defined as

$$h\left(\frac{z-b}{a}\right) = 1 \text{ for } b - a/2 \le z \le b$$
$$= -1 \text{ for } b \le z \le b + a/2$$
$$= 0 \text{ , otherwise}$$

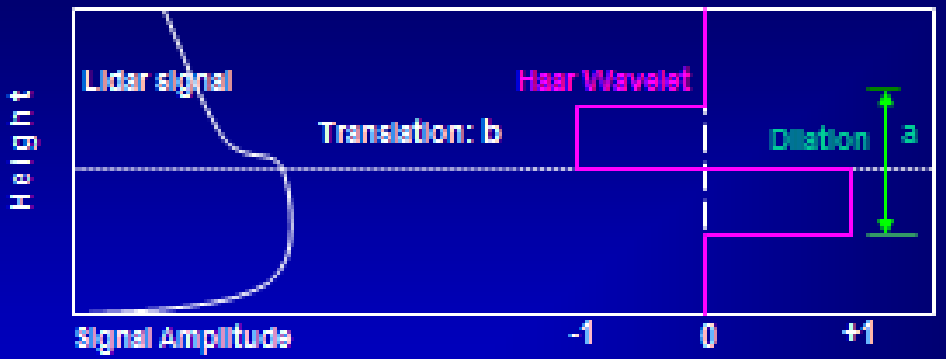

Equation: 2

$$W_f(a,b) = \frac{1}{a}\int_{Z_a}^{Z_b} \left\{ f(z)h\left(\frac{z-b}{a}\right)\right\} dz$$

Equation: 3

$$D^2(a) = \int_{Zb}^{Za} \left[W_f(a,b)^2\right] db$$

Calculation of convolution of R-square corrected backscatter profile and the haar function

Equation 2

Obtain covariance transforms $W_f(a,b)$

Choose a dilation value and search for a maxima $W_f(a,b)$

Find Location of the maxima

Haar wavelet transform results

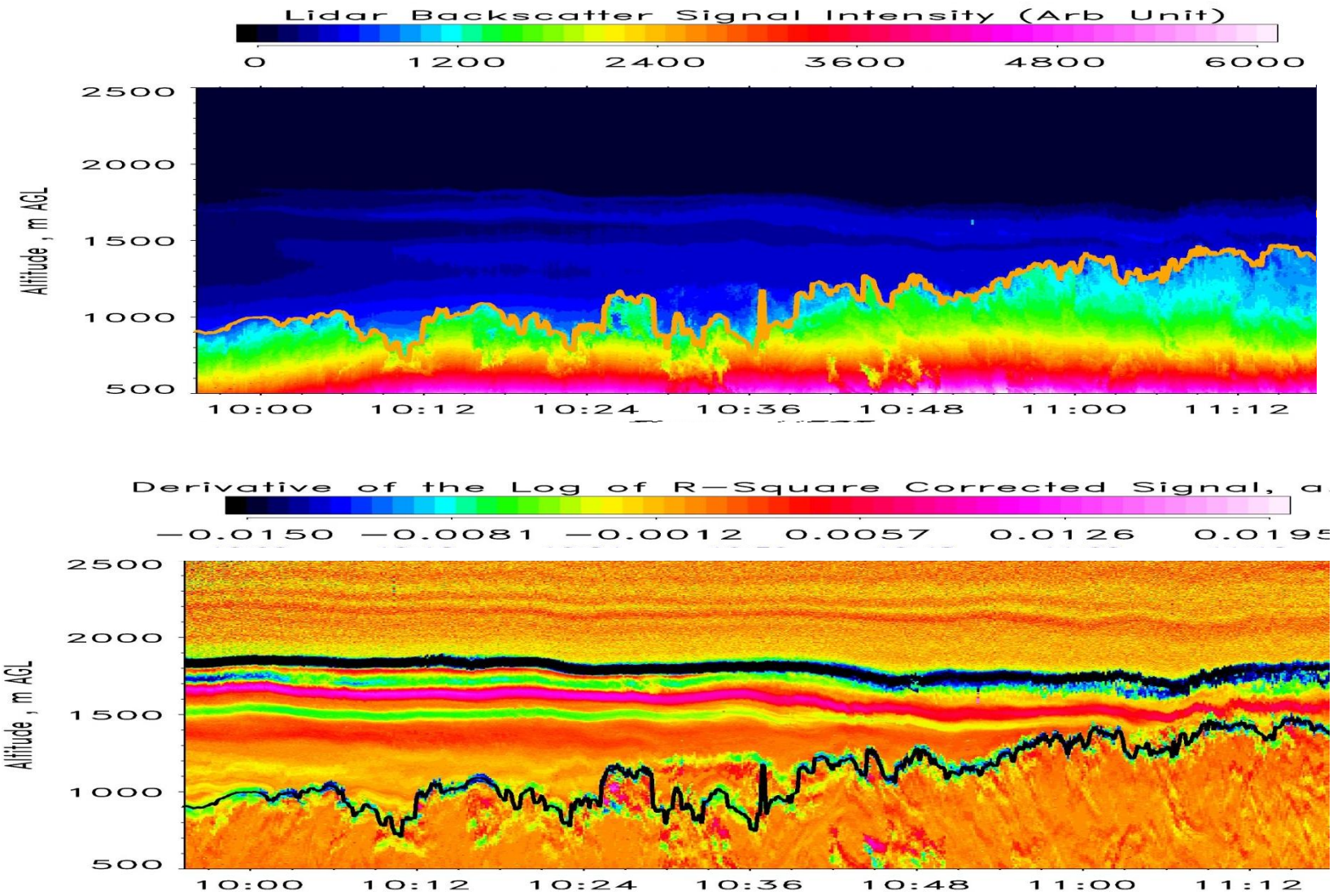

Wavelength: 1064 nm, Time resolution:0.33 s

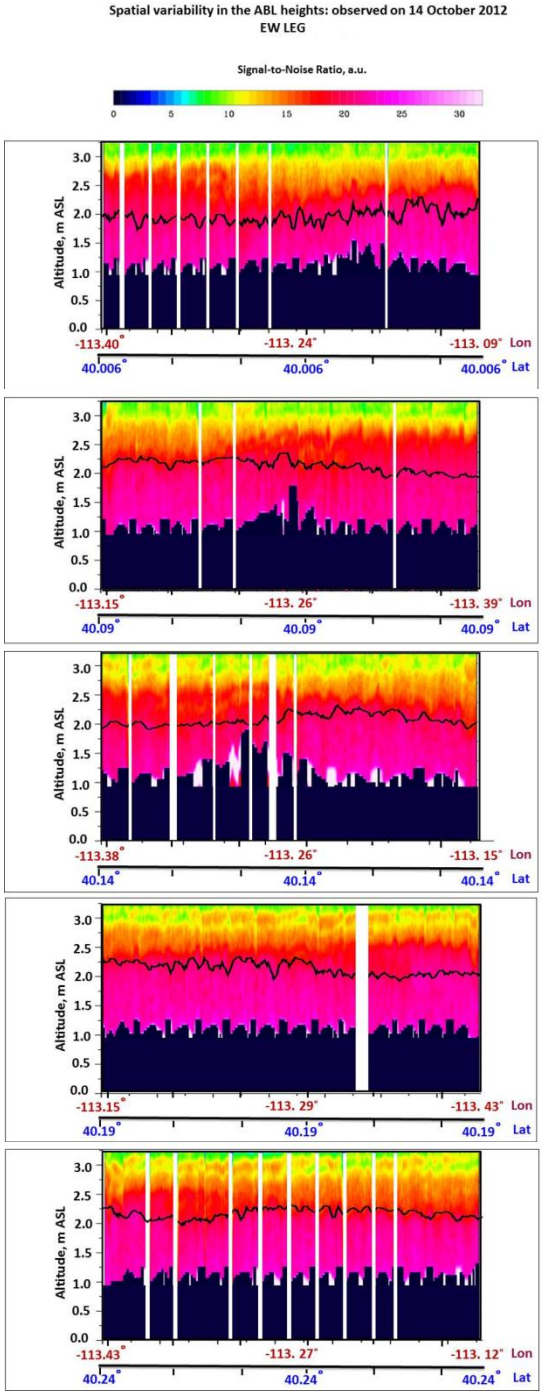

Generating 2D map providing spatial zi variability in a mesoscale domain

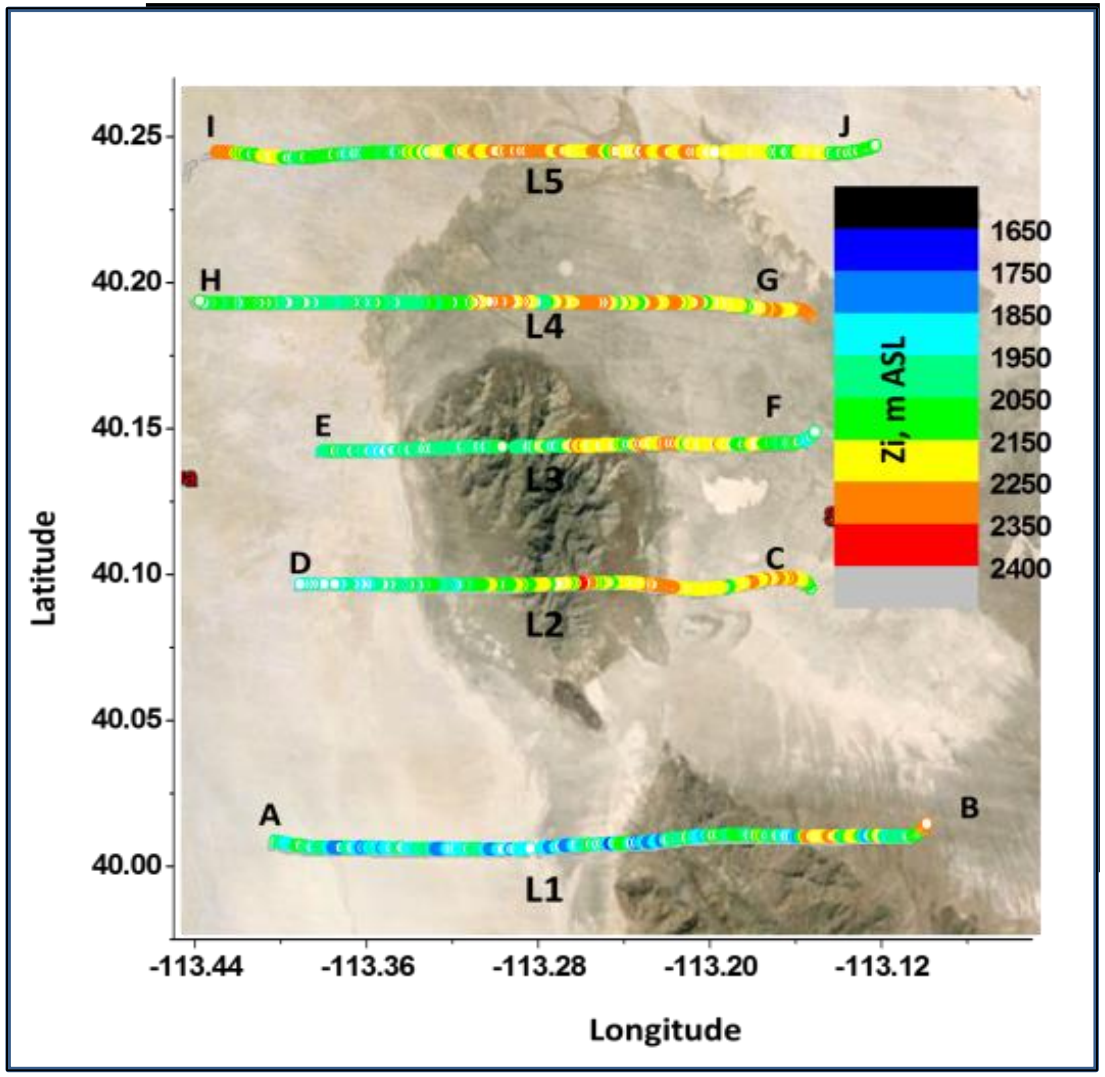

Radiosonde profiles of thermodynamic variables during selected IOPs

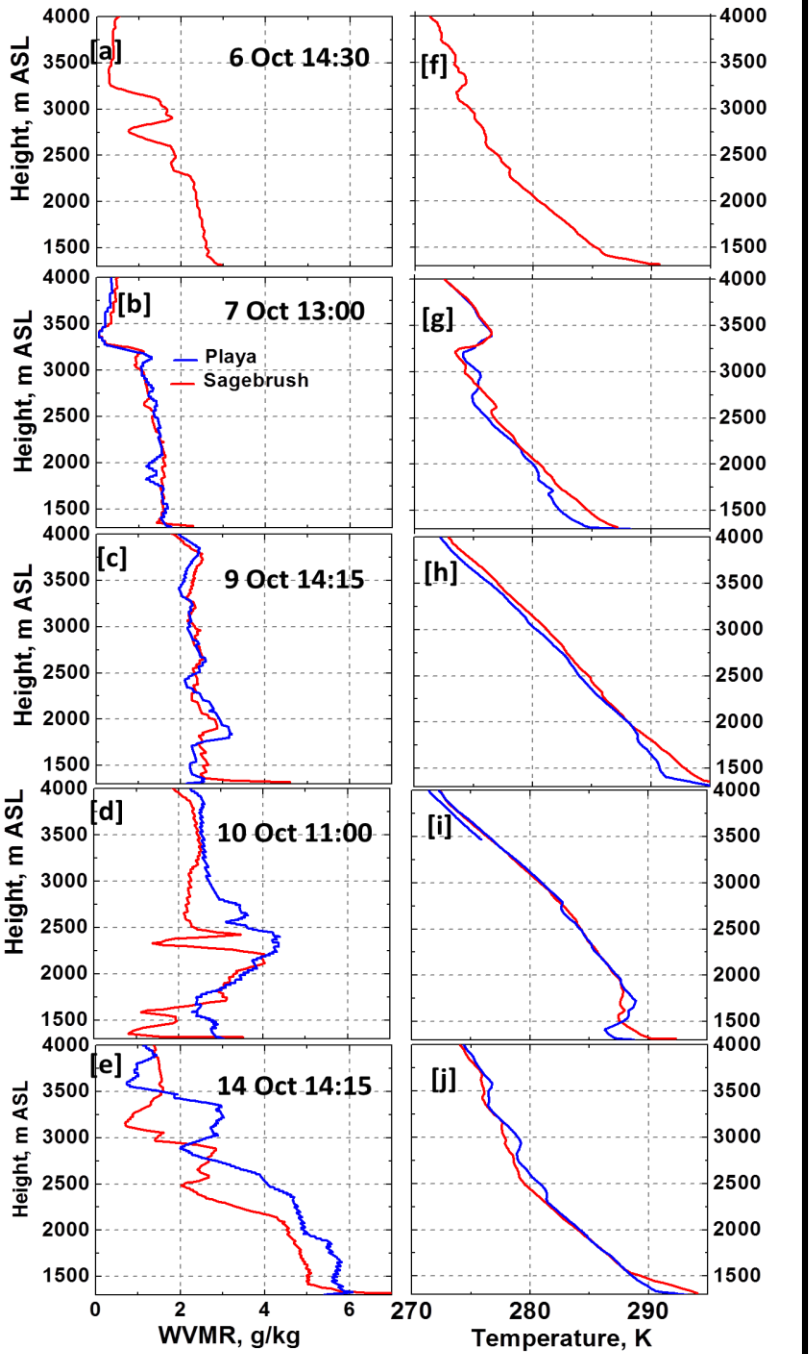

Intercomparison between radiosonde-derived profiles of water vapor mixing ratio (WVMR) ([a] to [e]) and temperature ([f] to [j]) over Sagebrush (red-solid line) and Playa (blue-solid line) sites during IOPs 4, 5, and 6.

Radiosonde profiles of zi during selected IOPs

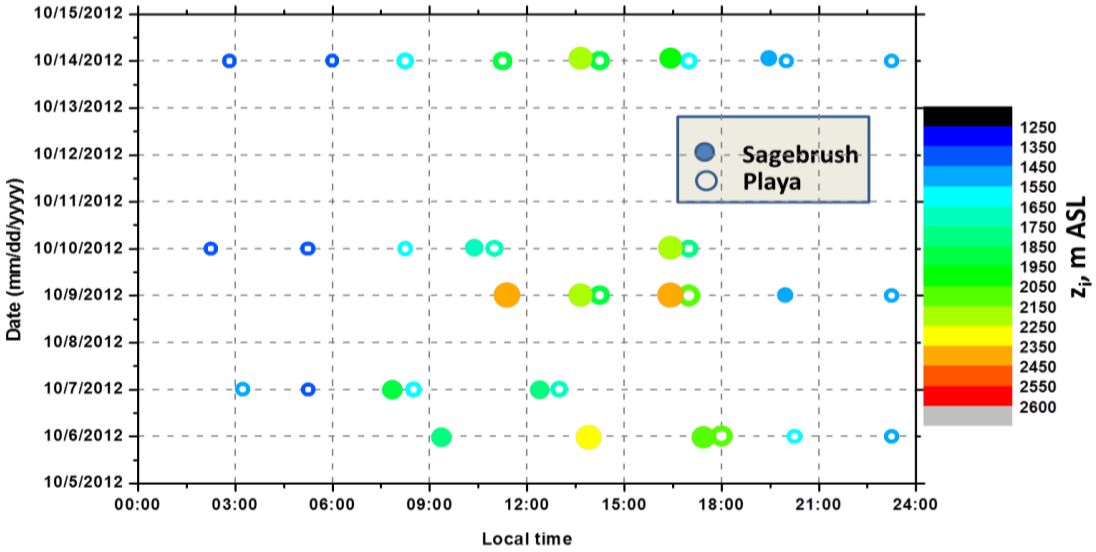

Radiosonde retrieved z_i over both eastern (filled circles) and western (open circles) sites during three IOPs. Color

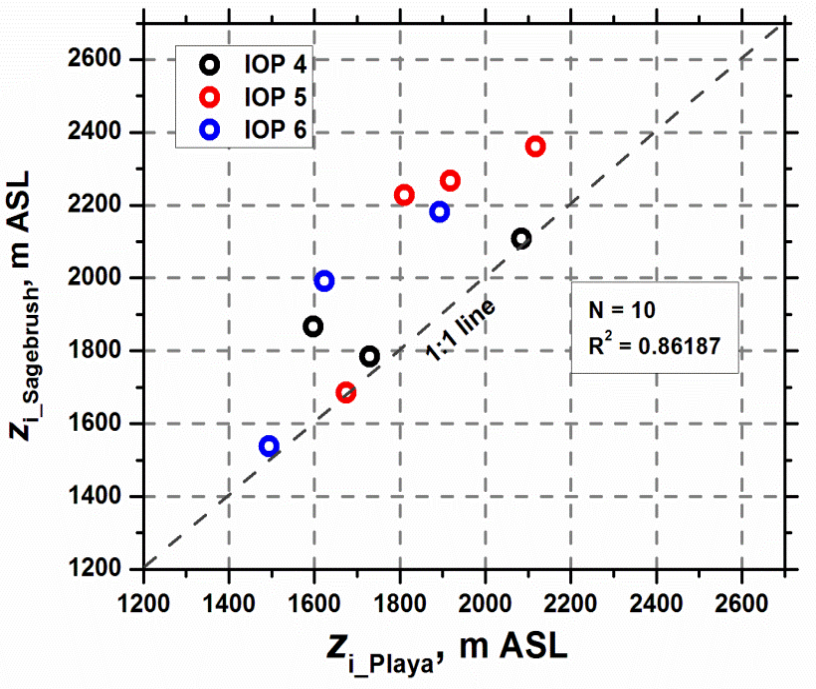

Intercomparison between $z_{i\_Sagebrush}$ and z_{i_Playa} retrieved from simultaneous radiosounding performed at both sites during IOP 4 (black circles), IOP 5 (red circles), and IOP 6 (blue circles).

TODWL derived CBL zi variability on 9 October 2012

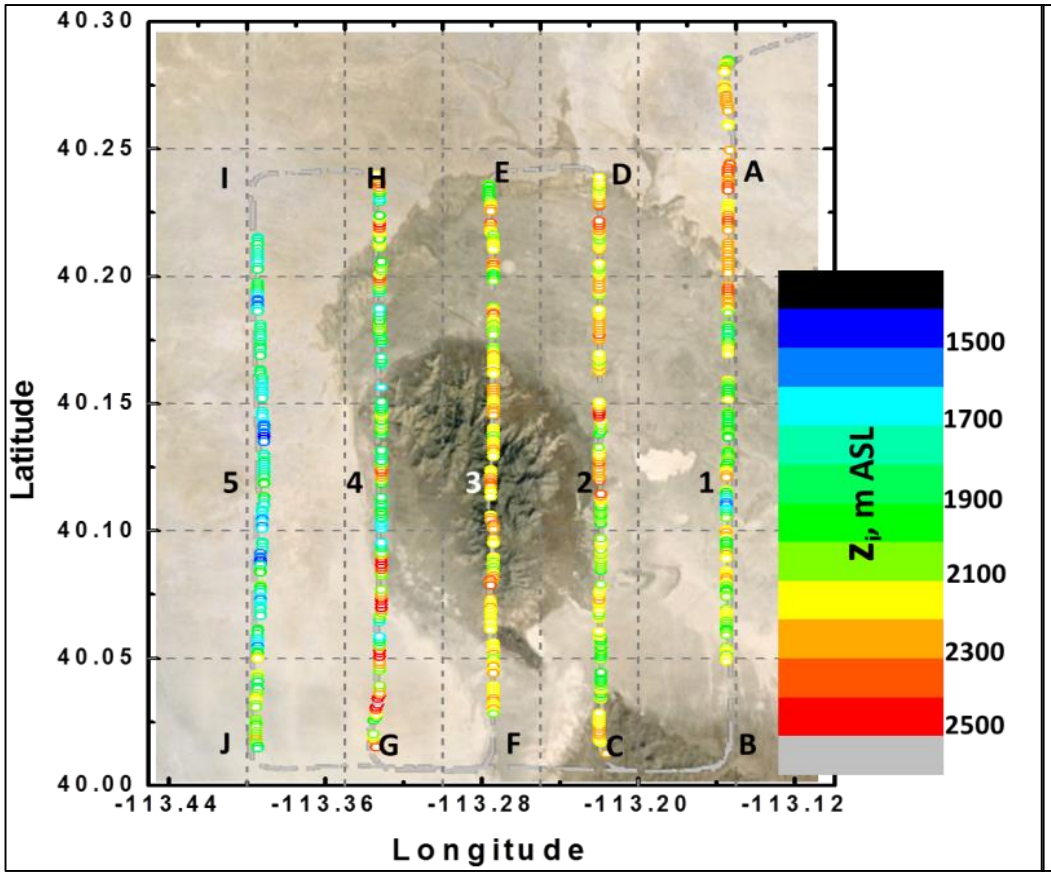

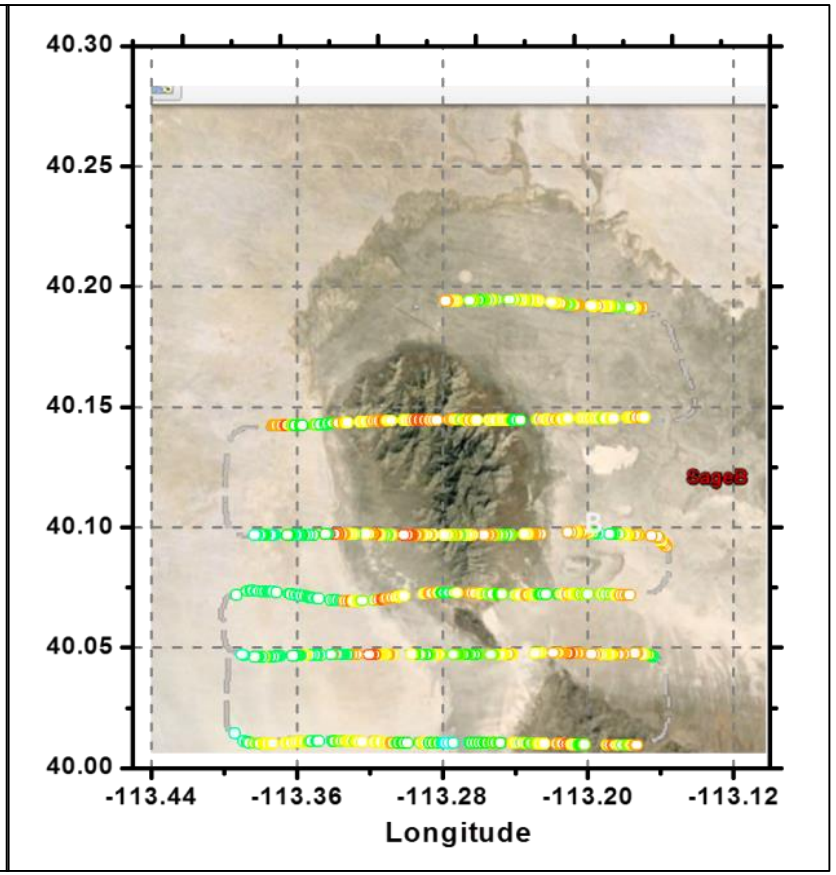

Observed z_i variability along the north-south and east-west legs during afternoon (from 16:00 to 17:15 LT) on 09 October 2012

TODWL derived CBL zi variability on 10 October 2012

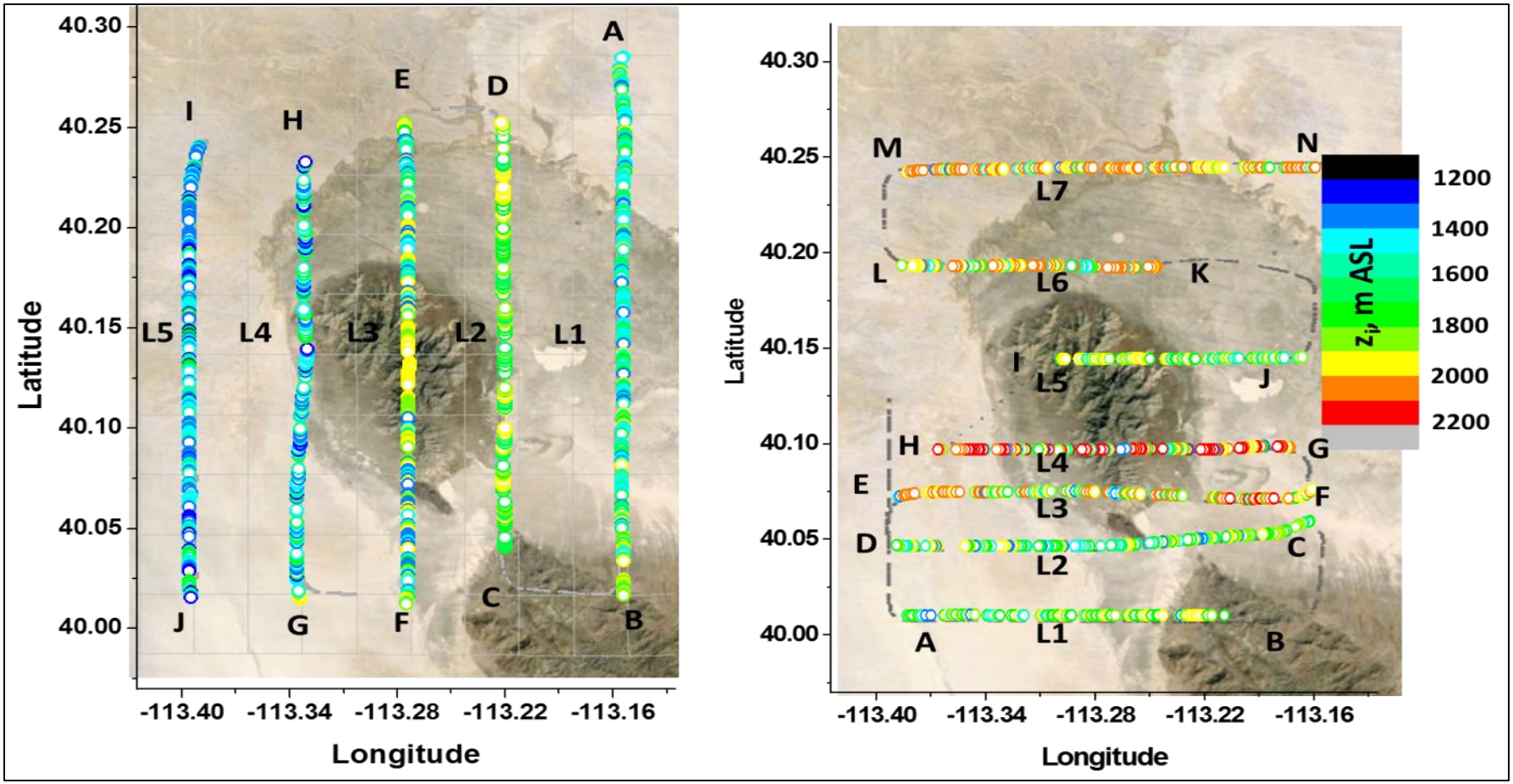

Observed z_i variability along 5 north-south and 7 east-west legs during morning (from 10:12 to 10:53 for NS legs, and from 10:54 to 11:37 for EW legs) on 10 October 2012.

TODWL derived CBL zi variability on 14 October 2012

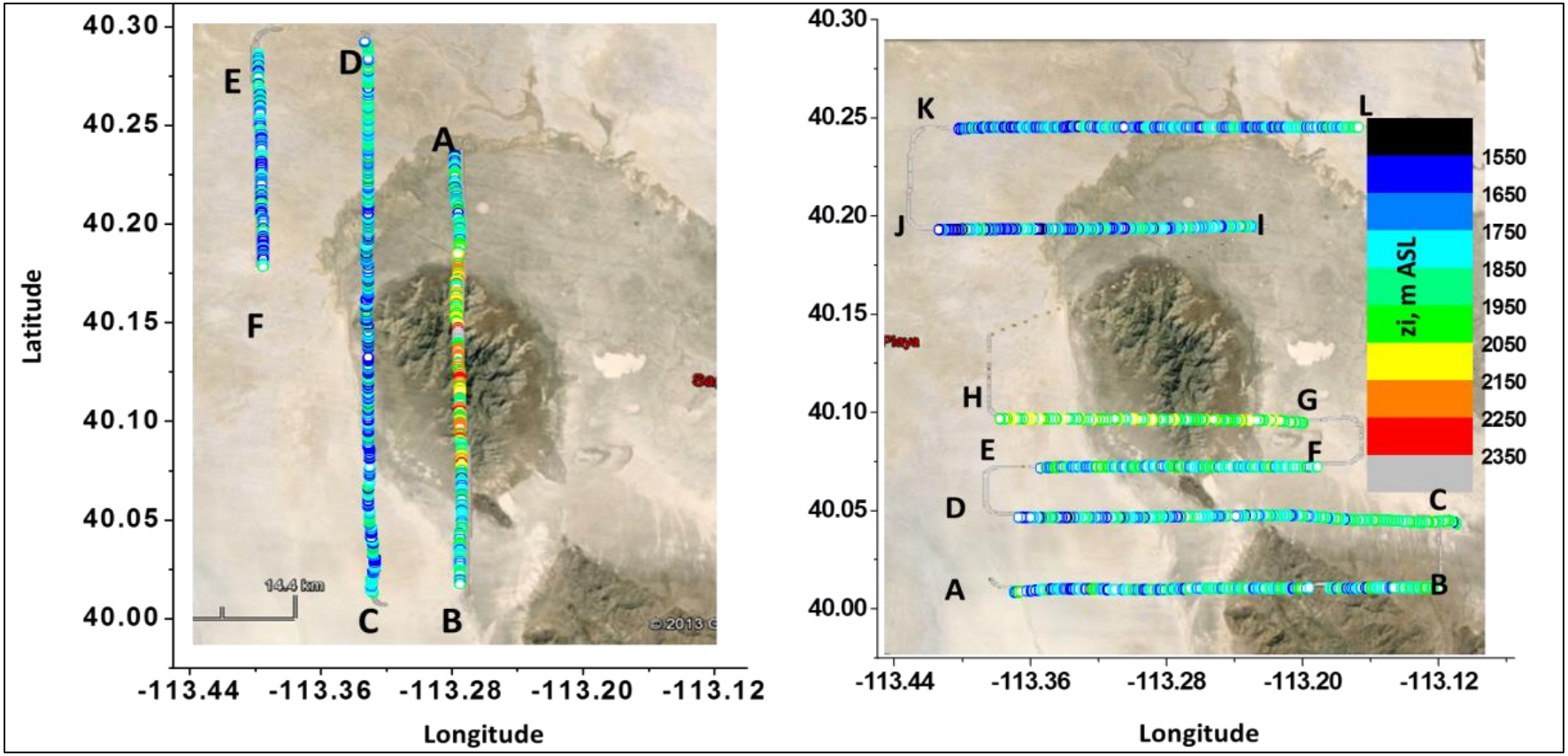

Observed z_i variability along the north-south and east-west legs on 14 October 2012 during morning (from 10:05 to 11:19) TOWDWL missions

TODWL derived CBL zi variability on 14 October 2012

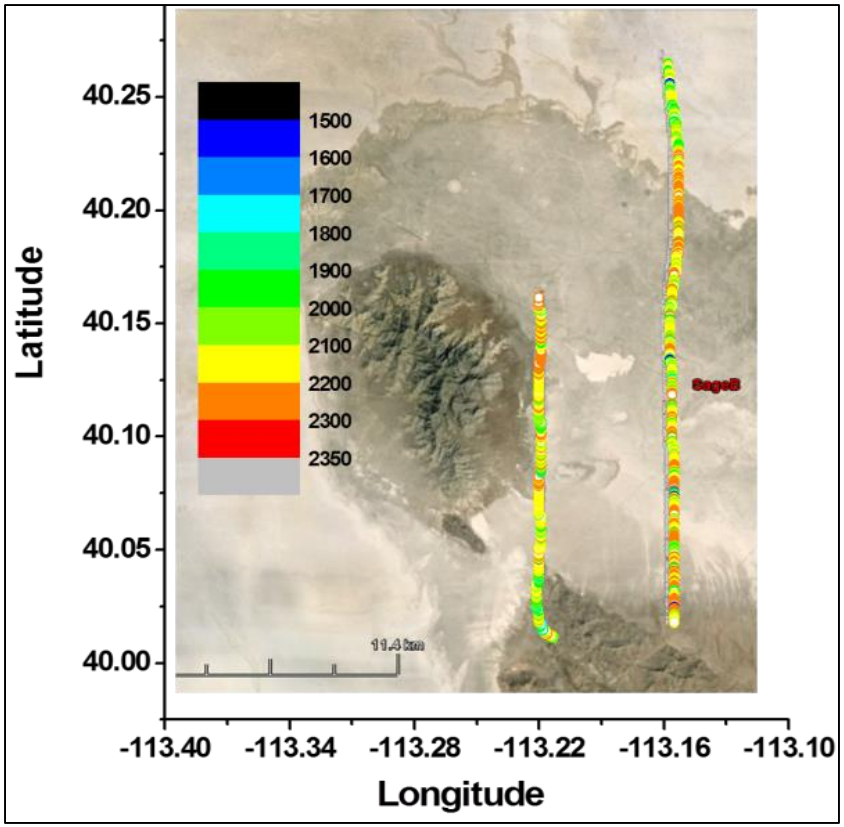

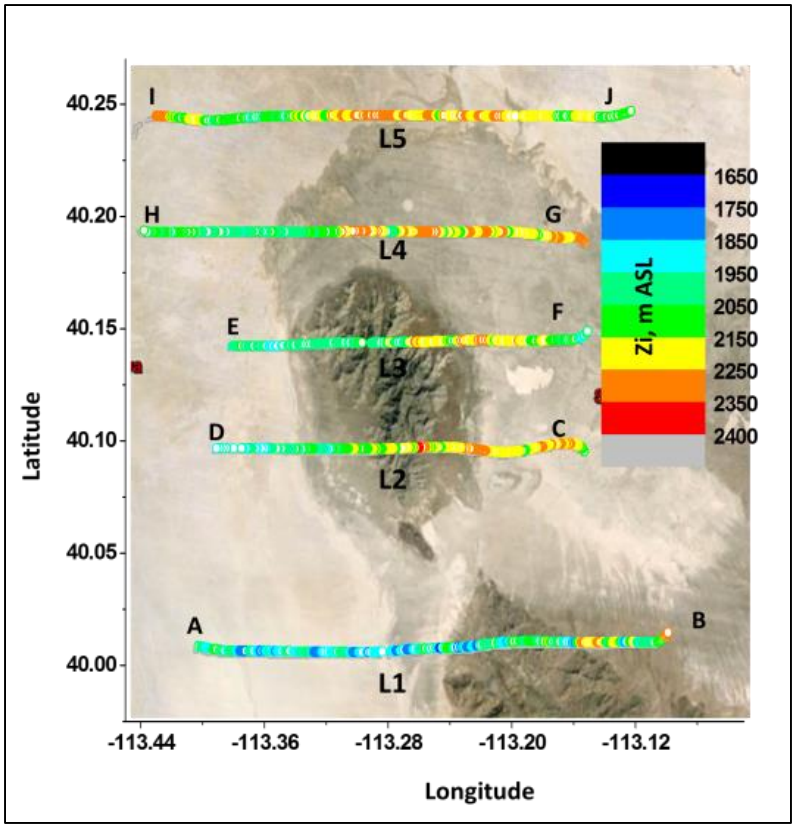

observed z_i variability along only east-west legs during afternoon between 16:05 and 16:46 LT on **14 Oct 2012**

Statistical analyses of TODWL derived CBL zi variability: NS legs

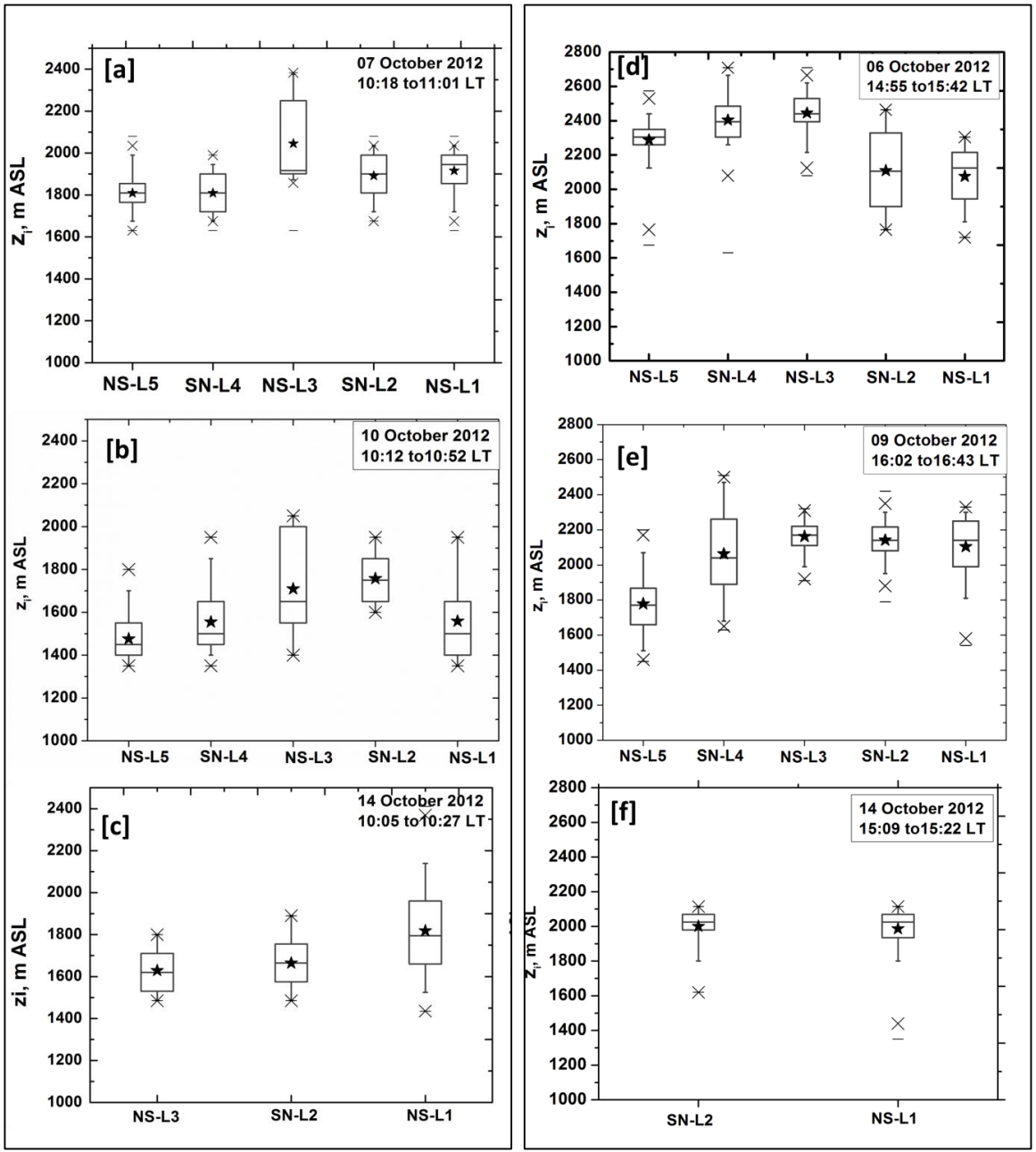

Box-and-whisker plots of z_i along the north-south flight legs performed on all three IOPs during morning

Statistical analyses of TODWL derived CBL zi variability: EW legs

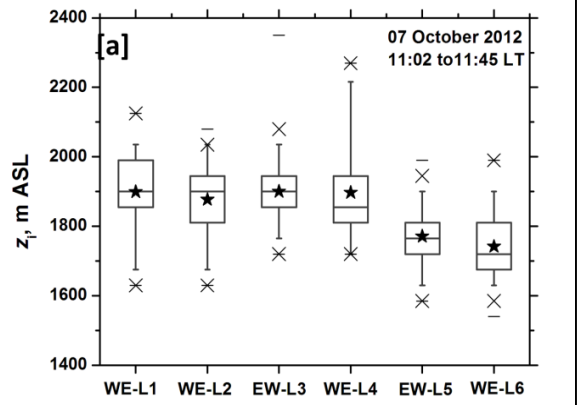

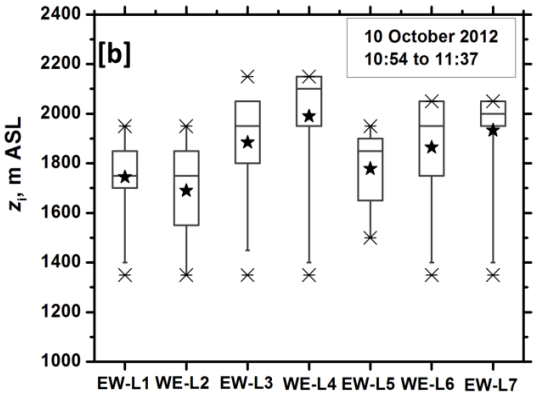

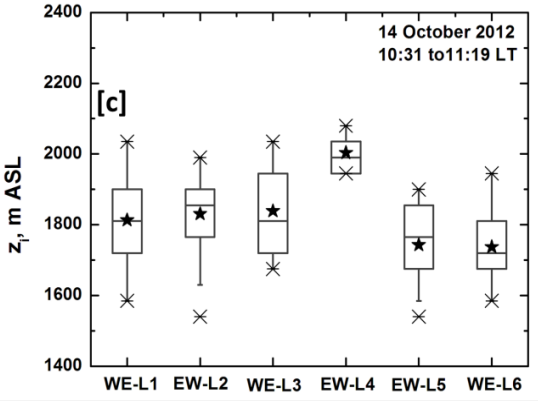

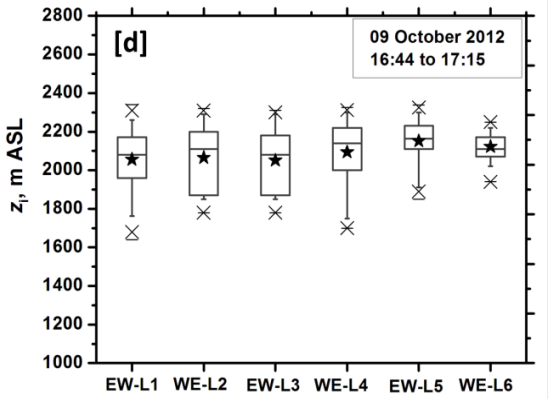

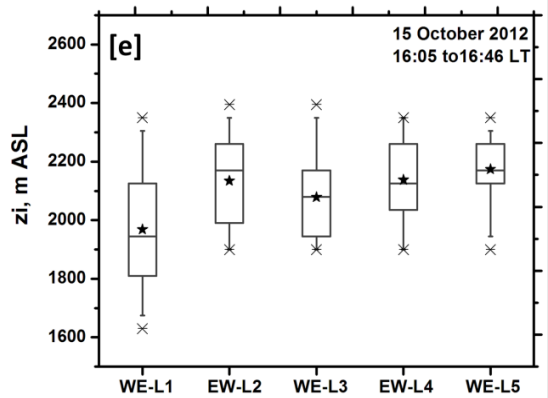

For east-west flight legs during three IOPs yielding NS zi variability

Day-to-day variability in near-surface meteorological parameters

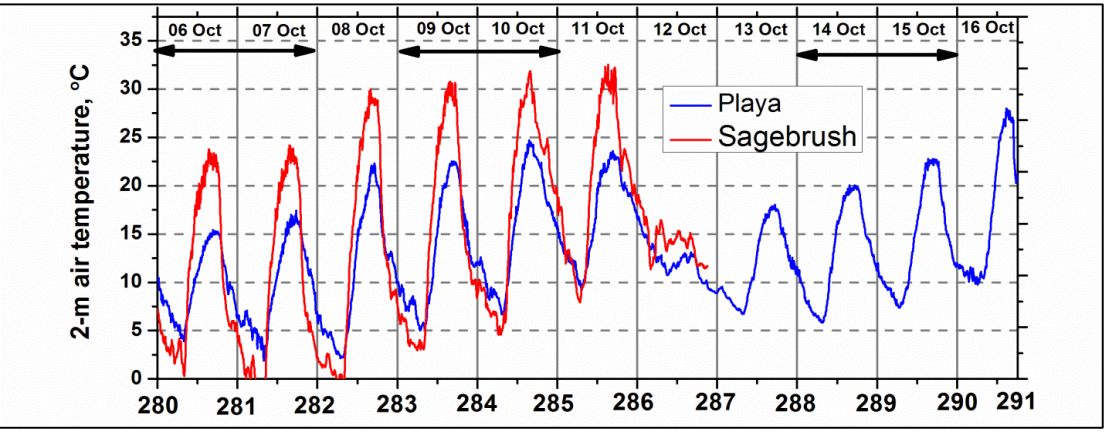

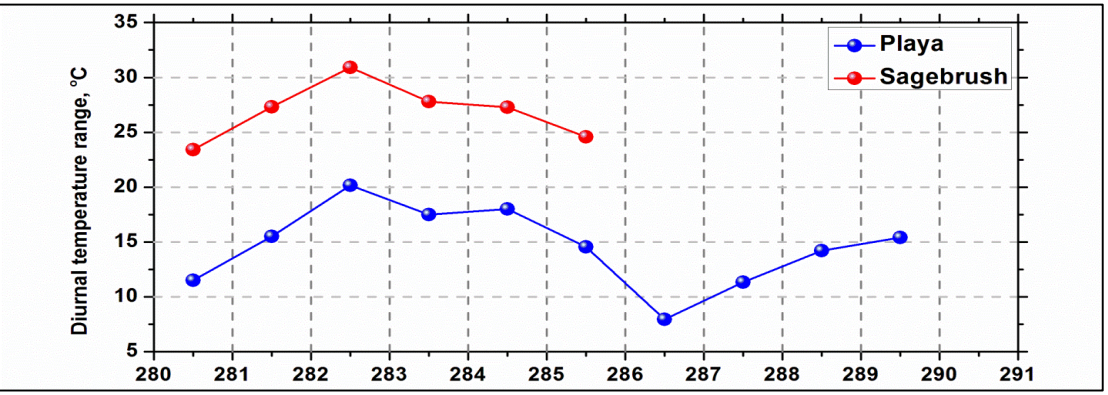

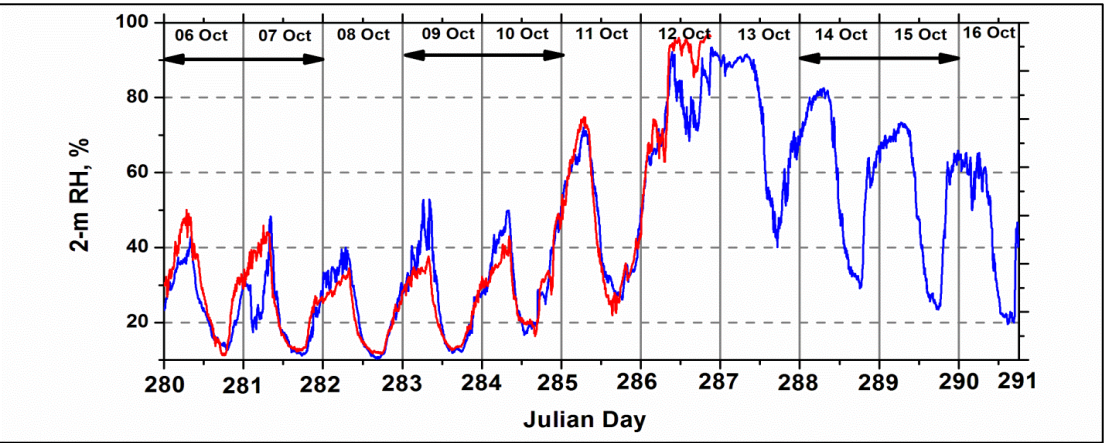

Day-to-day variability in the near-surface (2-m AGL) temperature (top), corresponding diurnal T, DTR, RH at both Sagebrush (red-solid line) and Playa (blue-solid line) sites from 06-16 October 2012.

Day-to-day variability in near-surface meteorological parameters

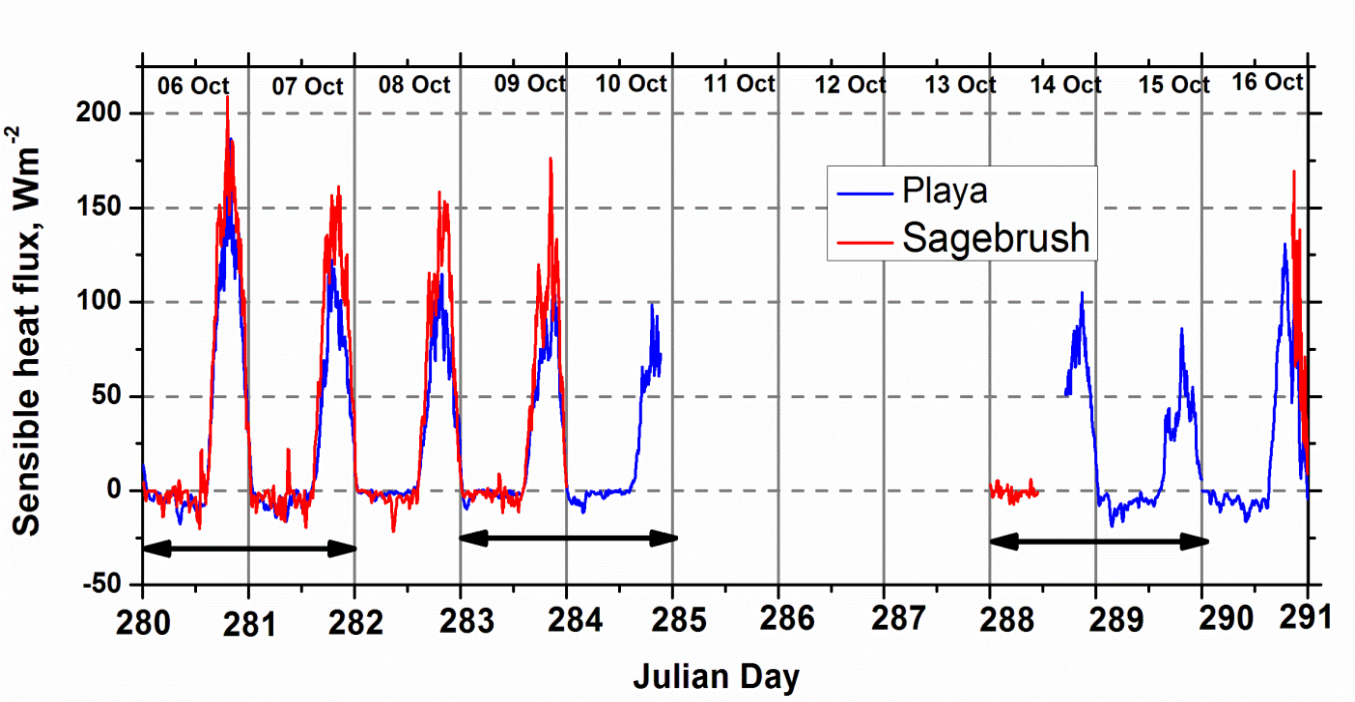

The diurnal course of near-surface (5 m AGL) sensible heat flux (in Wm^{-2}) at both Playa (blue-solid line) and Sagebrush (red-solid line) sites during the three selected IOPs marked by horizontally aligned arrows in both panels. Large differences in sensible heating lead to differences in boundary layer regimes over two sites.

TODWL: Concurrent measurements of zi and surface T

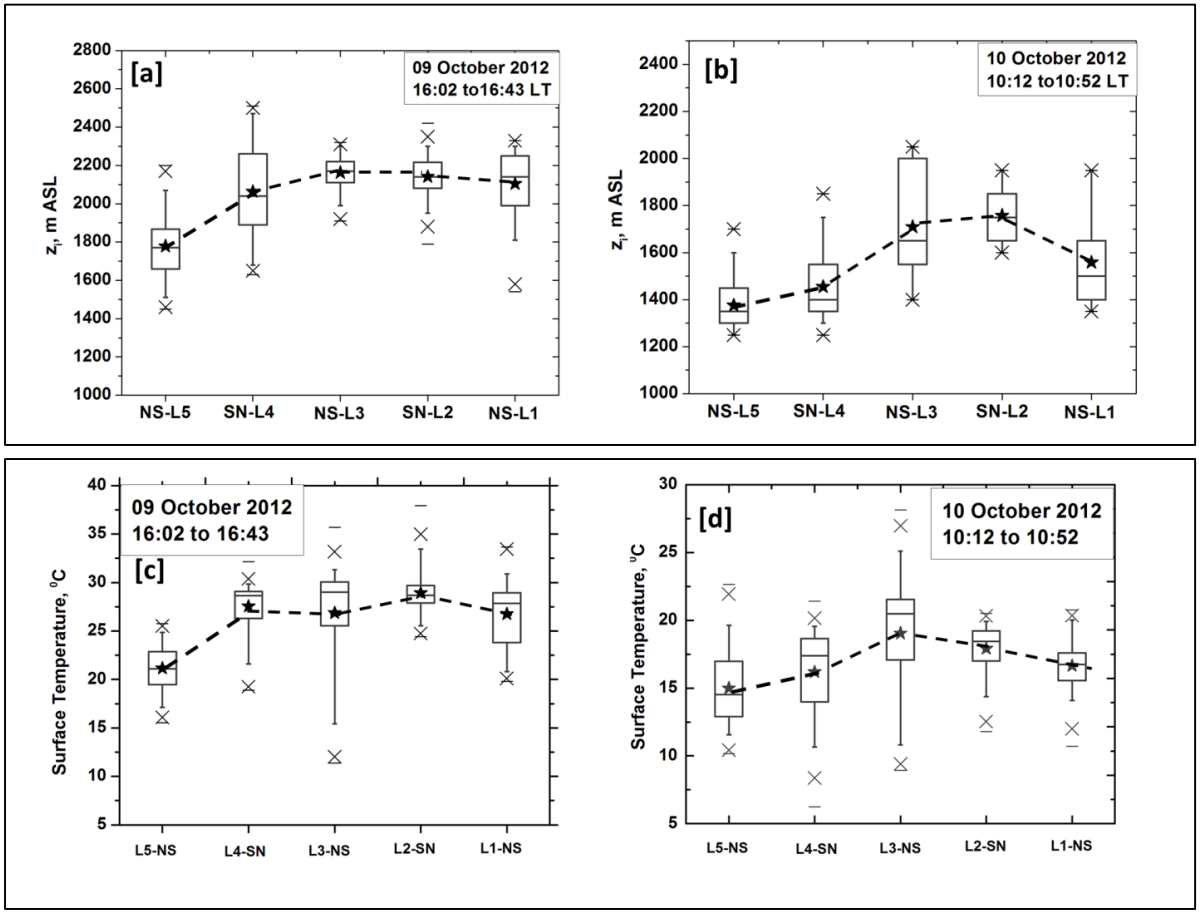

Box-and-whisker plots of z_i variability along NS flight legs on 09 (a) and 10 October (b). Lower panels: same as upper panels but for surface temperature measured by infrared temperature sensor from TODWL

- Significant East-West ABL depth gradient exists
- Well-mixed regimes exist
- NS legs over Granaite did not evince terrain following characteristics

- Along the NS leg over Granite: Terrain following feature observed
- Little East-West ABL depth gradient exists: Note BL did not grew fully during this time
- Cross-leg feature shows: Also local ABL and hence high ABL depths over Granite peak

Spatial zi variability with Manned and Unmanned Profilers

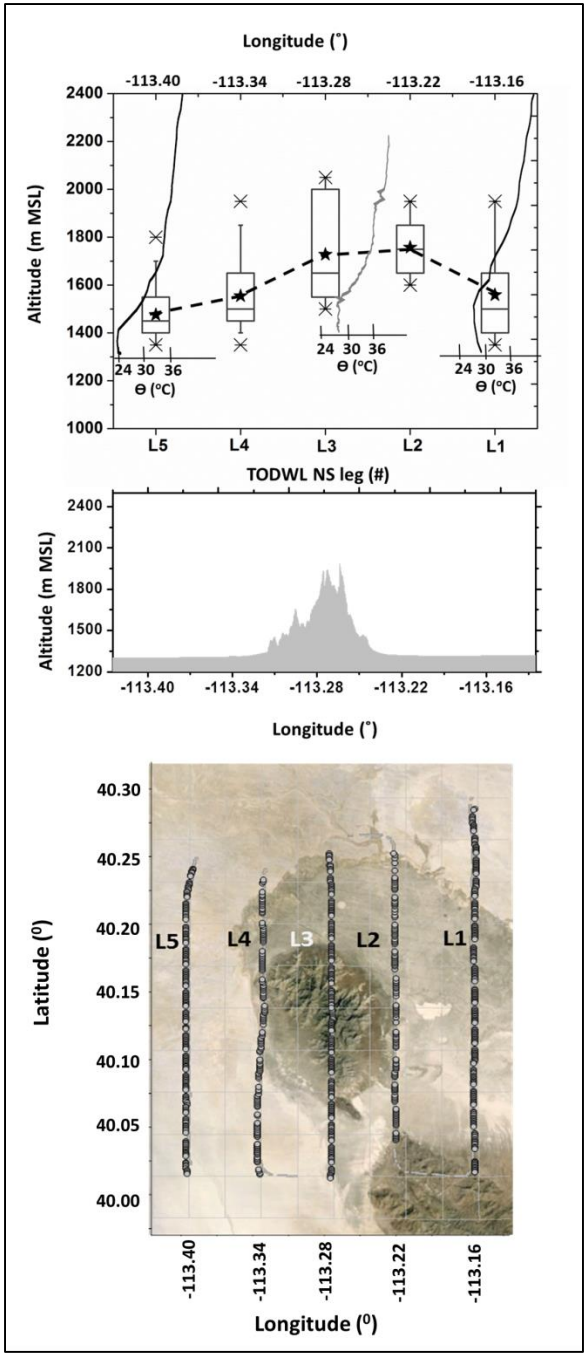

Box-and-whisker plot of CBL heights (above MSL) derived from aerosol backscatter profiles along the north-south TODWL flight legs during a morning mission between 1012 and 1052 MDT on 10 October 2012.

Statistical summary of TODWL derived CBL zi variability: EZT

Date and IOP #	Local time	Leg # & orientation	Mean z_i, m ASL	σ_{zi}, m	Measure of EZT	Skewness S_{zi}
06 October (IOP 4-RF 01)	14:55 to 15:42	NS-L1	2075	158	158	-0.329
		SN-L2	2109	237	237	0.049
		NS-L3	2445	117	117	-0.498
		SN-L4	2404	131	131	-0.521
		NS-L5	2287	112	112	-1.96
07 October (IOP 4-RF 02)	10:18 to 11:01	NS-L1	1915	85	NA	-0.853
		SN-L2	1892	96	NA	-0.246
		NS-L3	2045	193	NA	0.713
		SN-L4	1809	89	NA	0.265
		NS-L5	1809	93	NA	0.289
09 October (IOP 5-RF 03)	16:02 to 16:43	NS-L1	2104	168	168	-0.918
		SN-L2	2141	110	110	-0.299
		NS-L3	2163	88	88	-0.594
		SN-L4	2063	240	240	0.189
		NS-L5	1778	167	167	0.347
10 October (IOP 5-RF 04)	10:12 to 10:52	NS-L1	1558	180	NA	0.855
		SN-L2	1757	123	NA	0.254
		NS-L3	1709	234	NA	0.329
		SN-L4	1455	135	NA	0.997
		NS-L5	1375	100	NA	1.237
14 October (IOP 6-RF 05)	10:05 to 10:27	NS-L1	1970	211	NA	0.617
		SN-L2	1763	123	NA	0.200
		NS-L3	1728	104	NA	0.114
	15:09 to 15:22	NS-L1	2136	109	109	-2.34
		SN-L2	2150	98	98	-1.56

Findings and outlook

- Observations in the low isolated mountain showed that while the CBL structure in the morning is highly inhomogeneous, the afternoon CBL structure tends to be horizontally homogeneous

- Two different behaviors of the ABL: evolution of a CBL that follows the underlying terrain towards a CBL which seems to be unaffected by the terrain in homogeneity.

- RS-based observations also confirm the spatial variability in the ABL depths (WE gradient)

Findings and outlook

Multi-site multiple instruments: Two physical mechanisms

Impact of terrain heterogeneity on both morning and evening BL transitions

Topic 02: Impact of the terrain heterogeneity on both early morning and evening transitions

Practical Motivation: Demonstrate existing methodologies to define the EMT and the EET periods at selected sites that are perturbed by nearby complex terrains. Concurrent lidar/ceilometer measurements help attribute the erosion of the SBL inversion as well as the development of the SCBL (shallow convective boundary layer)

Scientific issues/questions

1. Defining both early morning and evening transition periods: searching and selecting a method among the methods available in the literature (inflection point in the near-surface temperature, boundary layer dilution effect in the water vapor mixing ratio, crossover by the SHF, and onset by stability parameters z/L etc.)
2. How do the collocated lidar/ceilometer measurements assist the attribution of the transition periods?
3. Applying a unified definition on the measurements obtained at three/four sites, can we illustrate the impact of flow features (on EET and EMT) that are generated due to the mountains in the area?

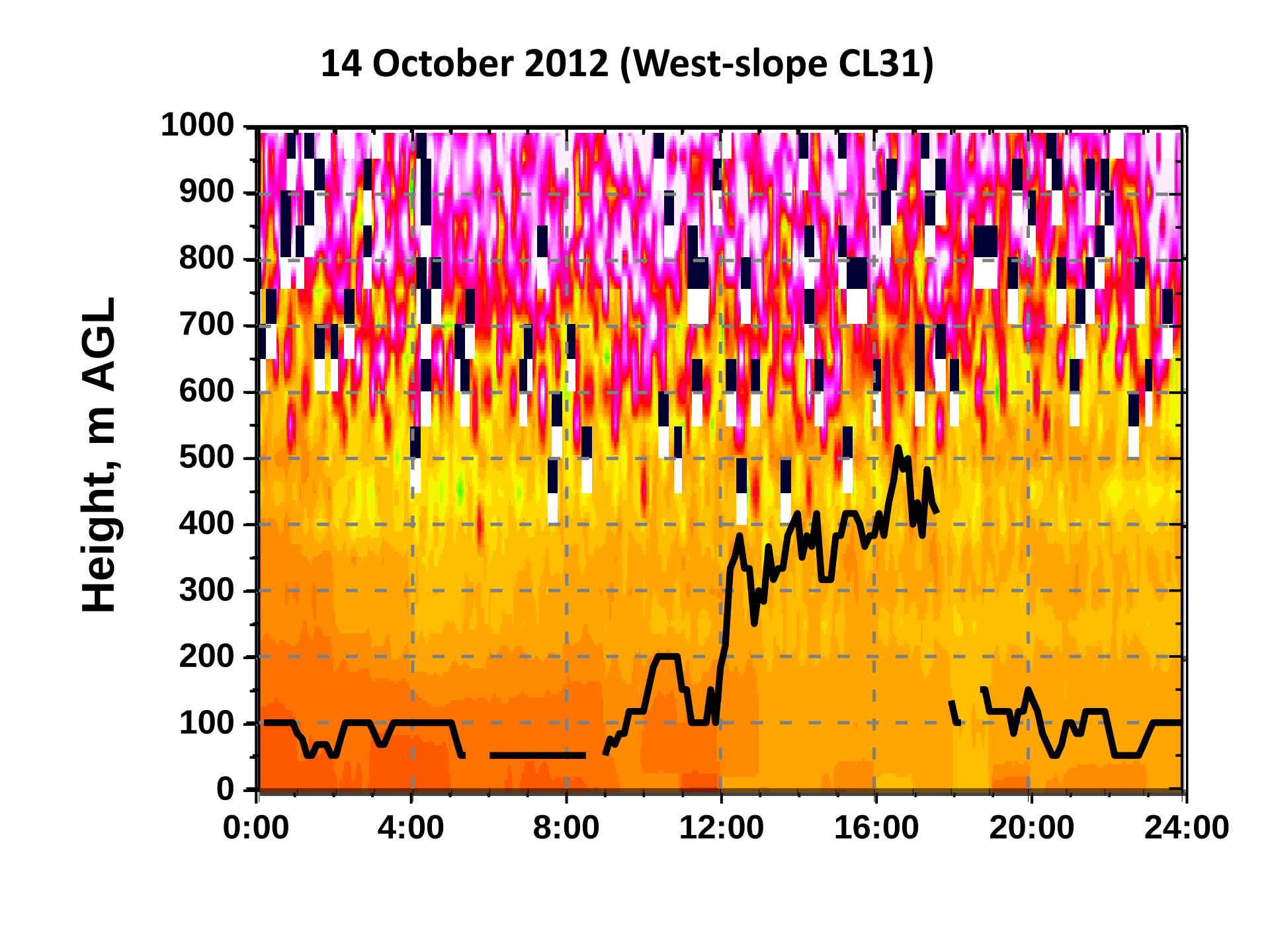
14 October 2012 (West-slope CL31)
Height, m AGL
1000
900
800
700
600
500
400
300
200
100
0
0:00
4:00
8:00
12:00
16:00
20:00
24:00

Thanks!
Danke!
Merci !

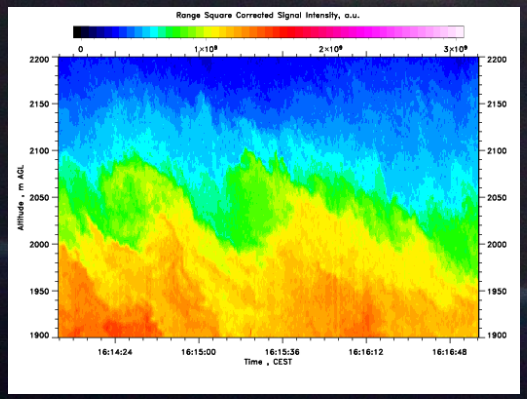

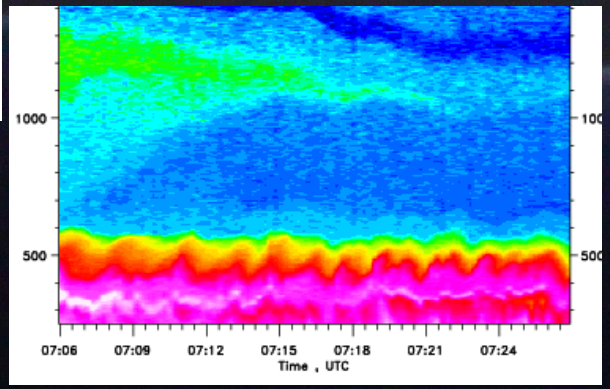

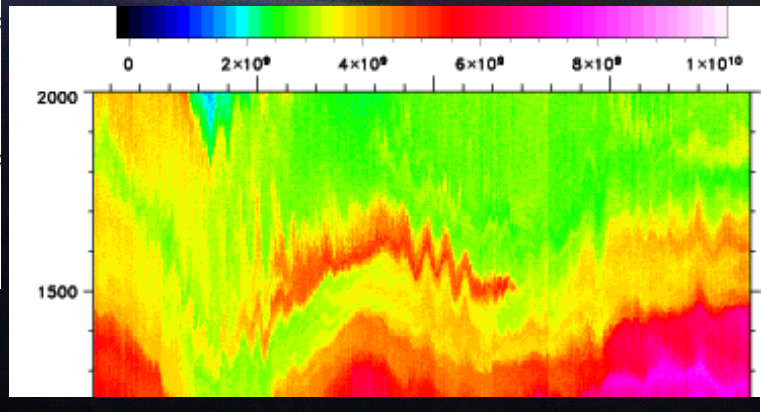

MATERHORN-X Fall - airborne

- Twin Otter in Utah between 5 October and 18 October, 2012, participated in 4 IOPs
- Missions lasted ~ 4 hours
- 7 research flights yielded ~3000 wind profiles between surface and 3400 m MSL

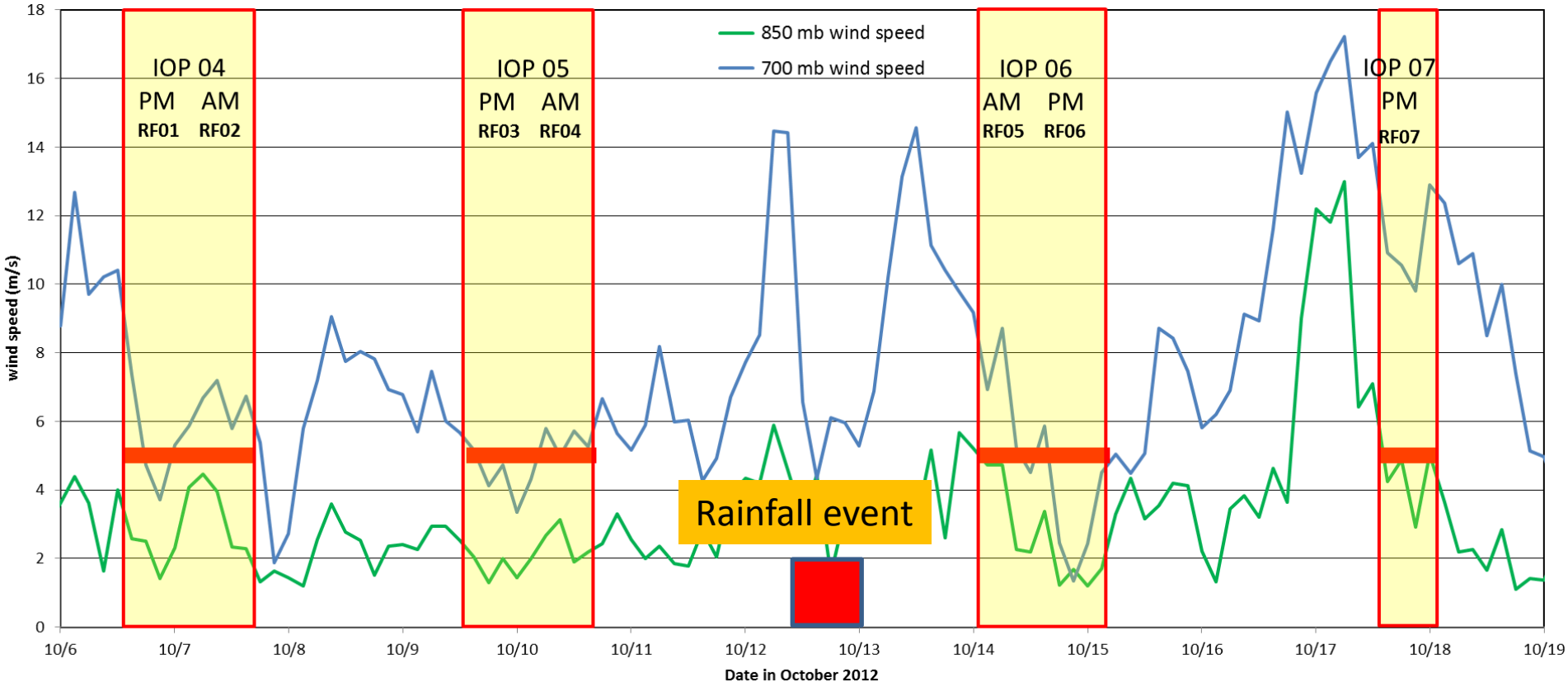

quiescent quiescent quiescent moderate

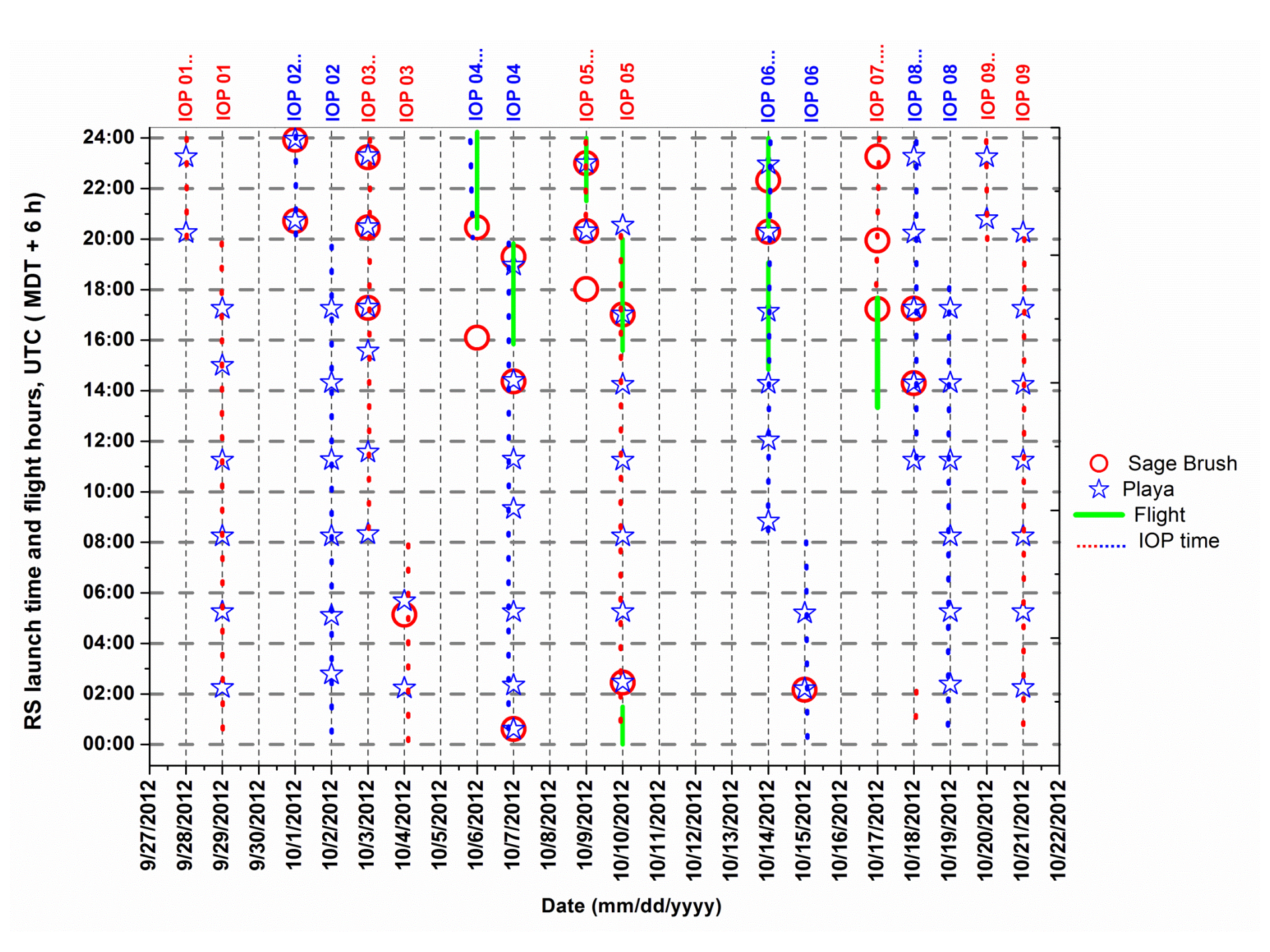
IOP 01..
IOP 01
IOP 02..
IOP 02
IOP 03..
IOP 03
IOP 04...
IOP 04
IOP 05...
IOP 05
IOP 06...
IOP 06
IOP 07....
IOP 08...
IOP 08
IOP 09..
IOP 09
RS launch time and flight hours, UTC (MDT + 6 h)
24:00
22:00
20:00
18:00
16:00
14:00
12:00
10:00
08:00
06:00
04:00
02:00
00:00
9/27/2012
9/28/2012
9/29/2012
9/30/2012
10/1/2012
10/2/2012
10/3/2012
10/4/2012
10/5/2012
10/6/2012
10/7/2012
10/8/2012
10/9/2012
10/10/2012
10/11/2012
10/12/2012
10/13/2012
10/14/2012
10/15/2012
10/16/2012
10/17/2012
10/18/2012
10/19/2012
10/20/2012
10/21/2012
10/22/2012
Date (mm/dd/yyyy)
Sage Brush
Playa
Flight
IOP time

A Classical Atmospheric Boundary Layer

Stull, 1988

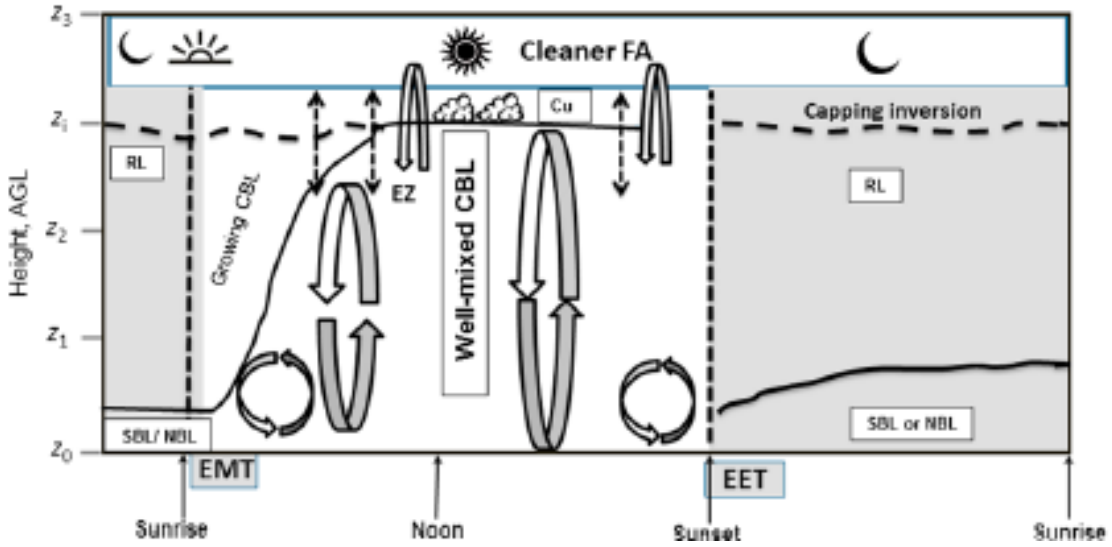

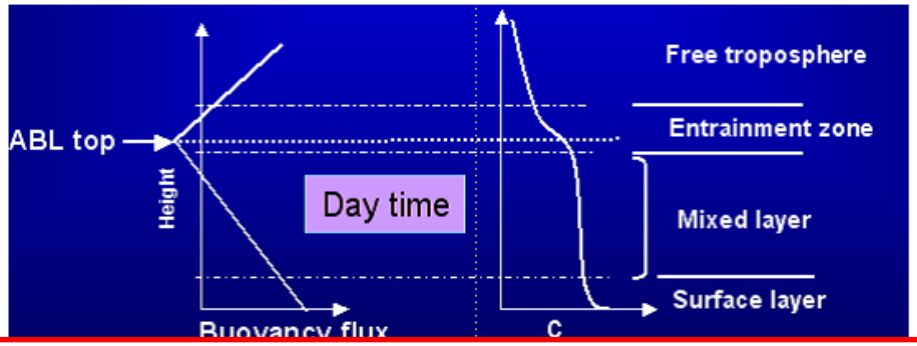

Monitoring of the ABL is an urgent issue
Largest variability contrary to any other part of the earth's atmosphere
Majority of the sources and sinks are located in the ABL.

Aerosol distribution and aerosol transport processes in the ABL in urban regions
Large pollution events for various anthropogenic activities

Wrong simulation of the ABL, entrainment zone, and residual layer including the diurnal/inter-diurnal development is crucial for the deficiencies in the numerical weather prediction models.

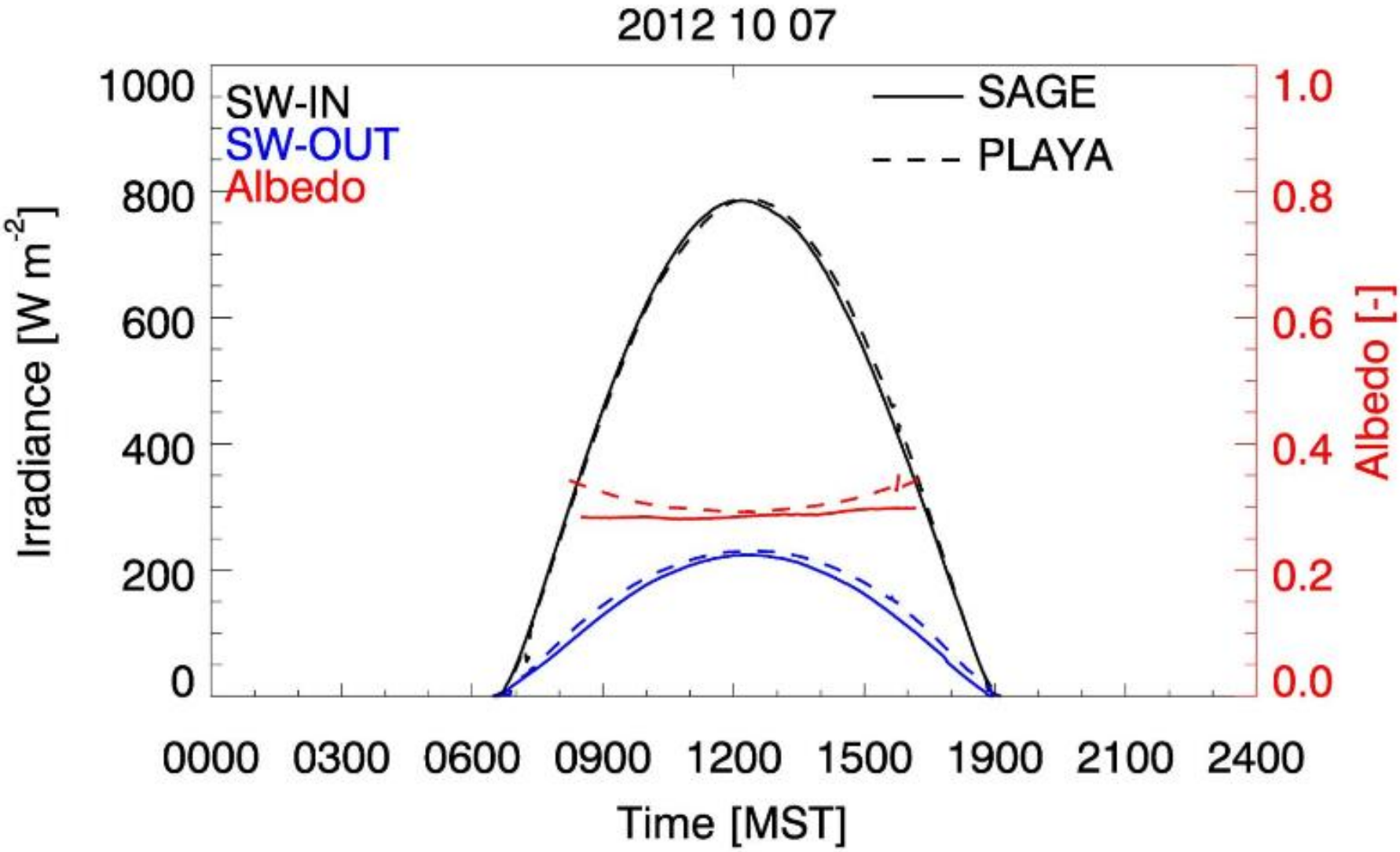
2012 10 07
SW-IN
SW-OUT
Albedo
SAGE
PLAYA
Irradiance [W m-2]
Albedo [-]
1000
800
600
400
200
0
1.0
0.8
0.6
0.4
0.2
0.0
0000
0300
0600
0900
1200
1500
1900
2100
2400
Time [MST]

MATERHORN data analyses: UND Ceilometer west slope near playa

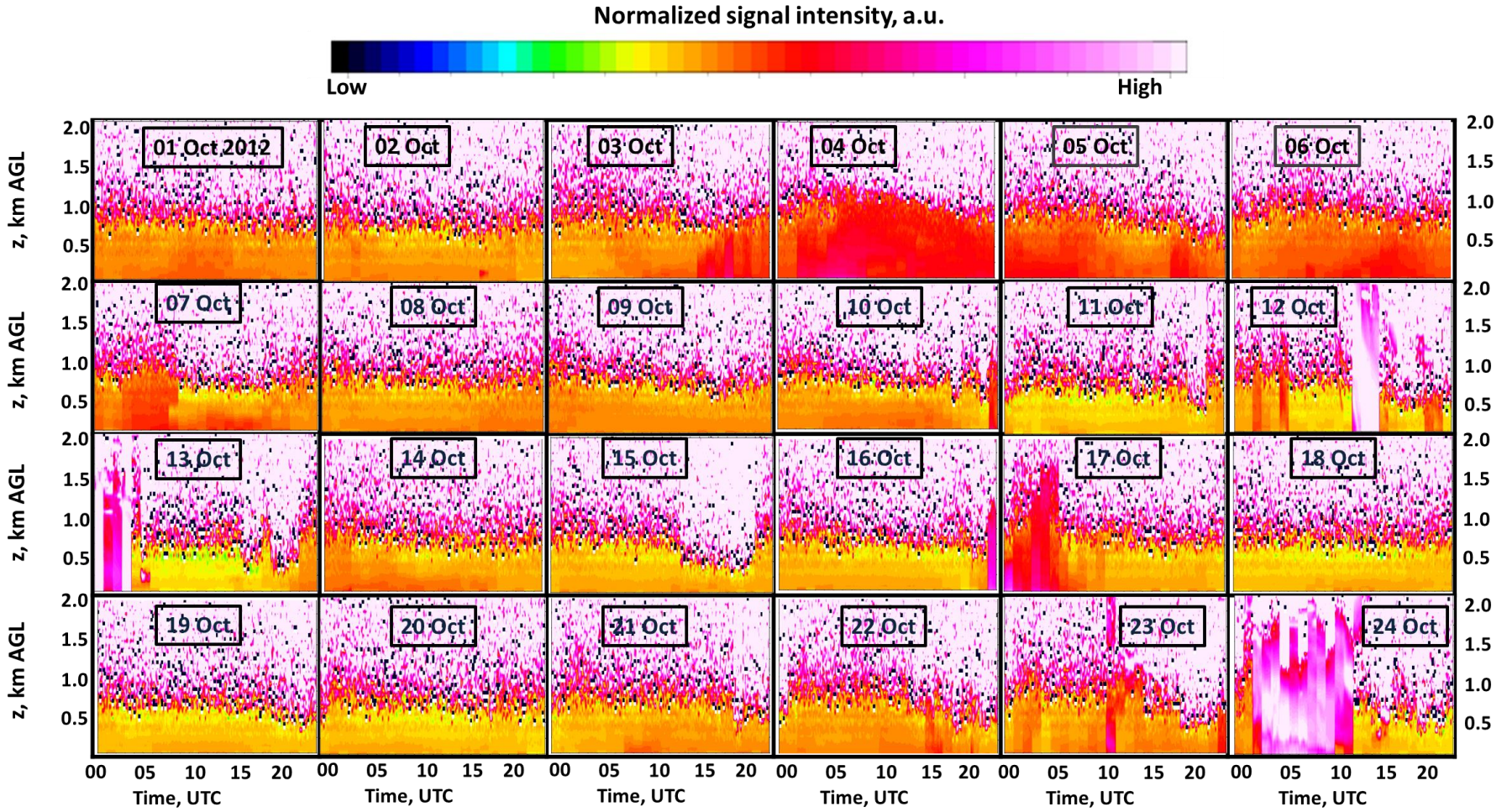

1. Instrument: UND Ceilometer, west slope near playa (40.101380, -113.337590, 1309.85 m ASL)
2. Plates of time-height cross-section of normalized signal intensity are shown to investigate aerosol stratification and boundary layer evolution during entire diurnal cycle during different days.
3. Temporal and spatial resolutions are 7.5 min and 50 m, respectively.
4. Time is in UTC, Height is in km above ground level (z, km AGL)
5. Moist elevated boundary layer (up to 1.2 km AGL) with high aerosol content within the ABL could be seen during the first one week of the experiment.
6. Precipitation signatures are well-observed during 12-13 Oct measurements. Also on 24 Oct!!
7. Last spell of the measurements show relatively drier ABL, however, needs to be confirmed.

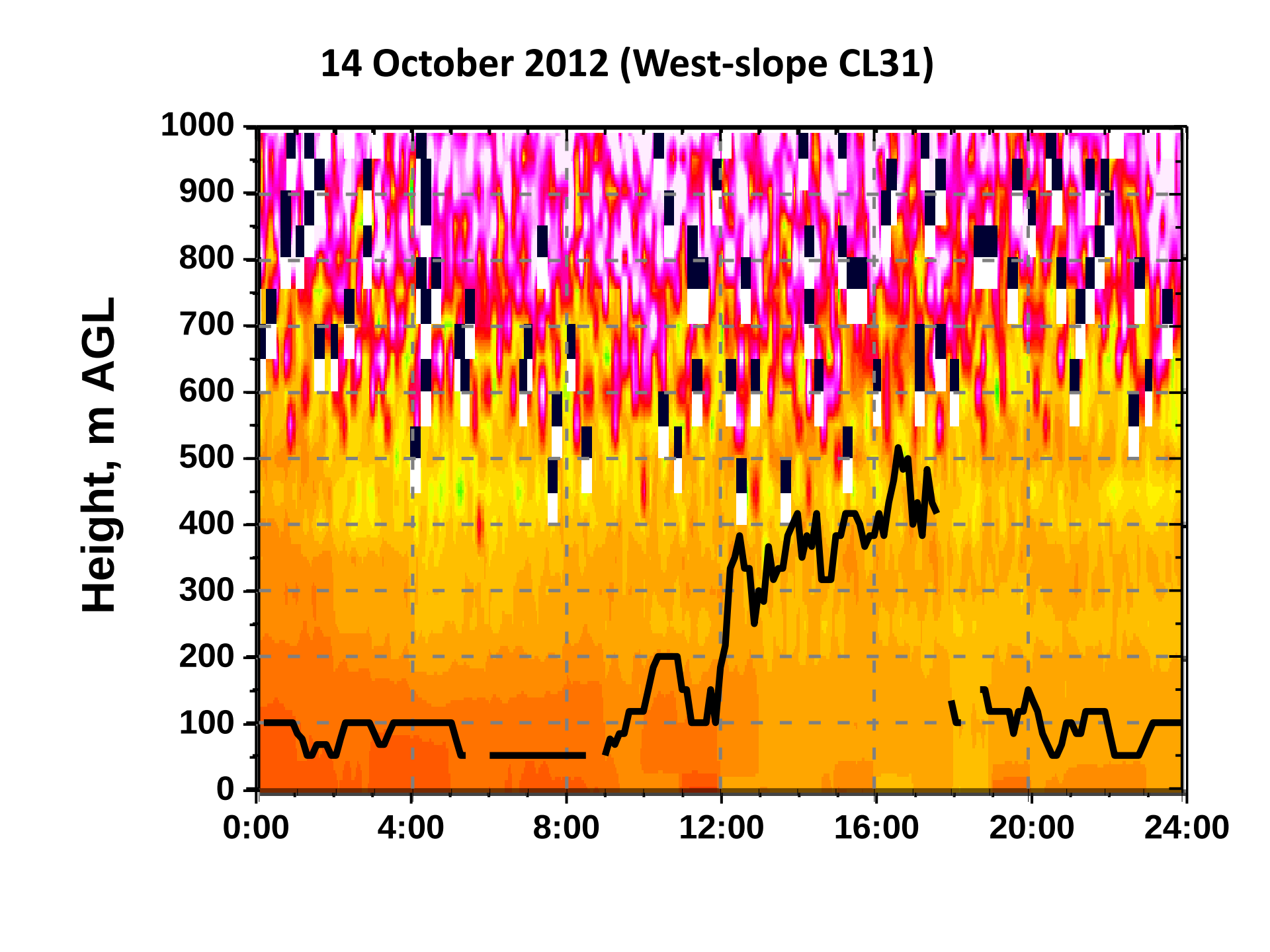
14 October 2012 (West-slope CL31)
Height, m AGL
1000
900
800
700
600
500
400
300
200
100
0
0:00
4:00
8:00
12:00
16:00
20:00
24:00

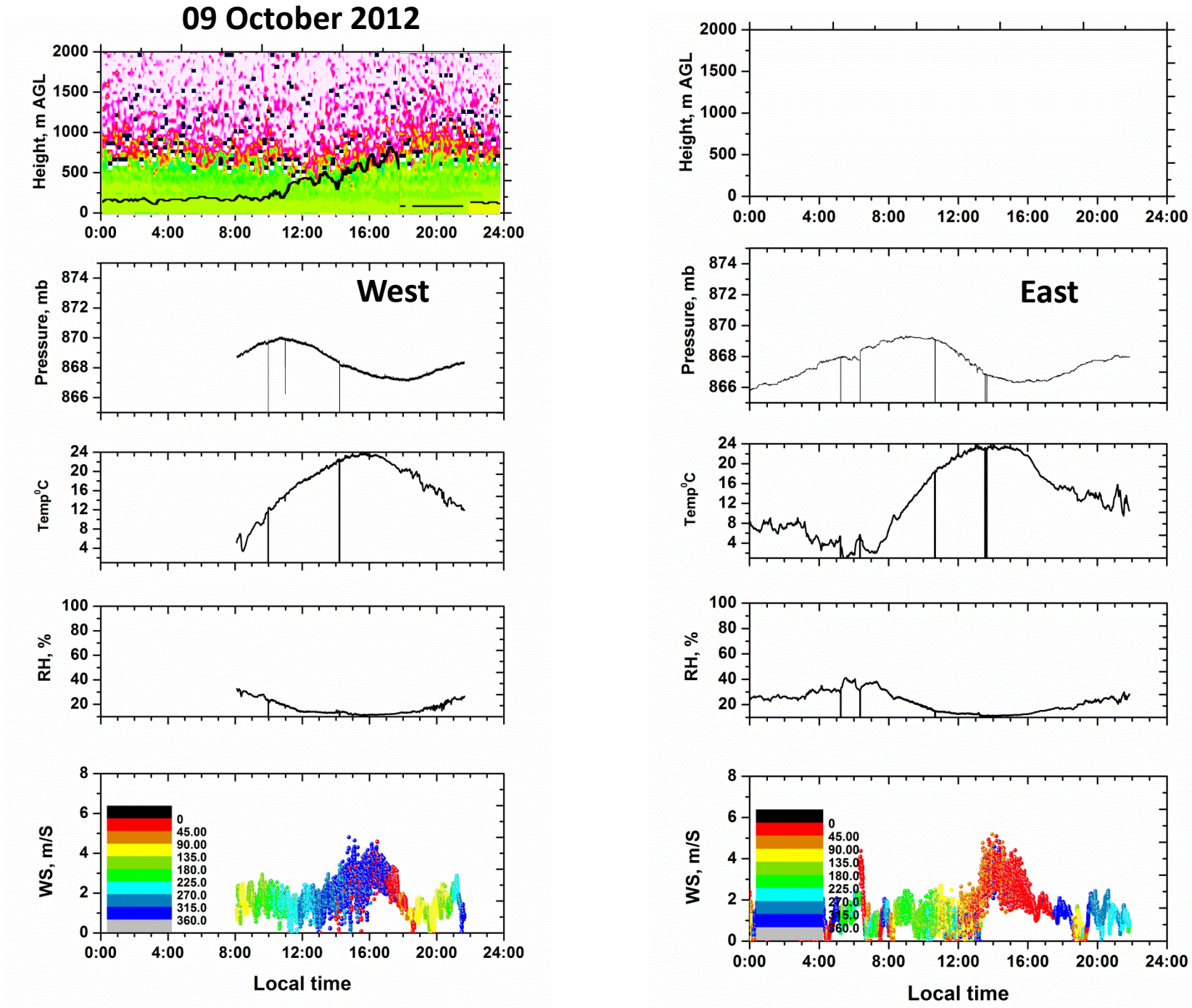
09 October 2012
Height, m AGL
2000
1500
1000
500
0
0:00
4:00
8:00
12:00
16:00
20:00
24:00
West
East
Pressure, mb
874
872
870
868
866
Temp°C
24
20
16
12
8
4
RH, %
100
80
60
40
20
WS, m/S
6
4
2
0
0
45.00
90.00
135.0
180.0
225.0
270.0
315.0
360.0
Local time

10 October 2012

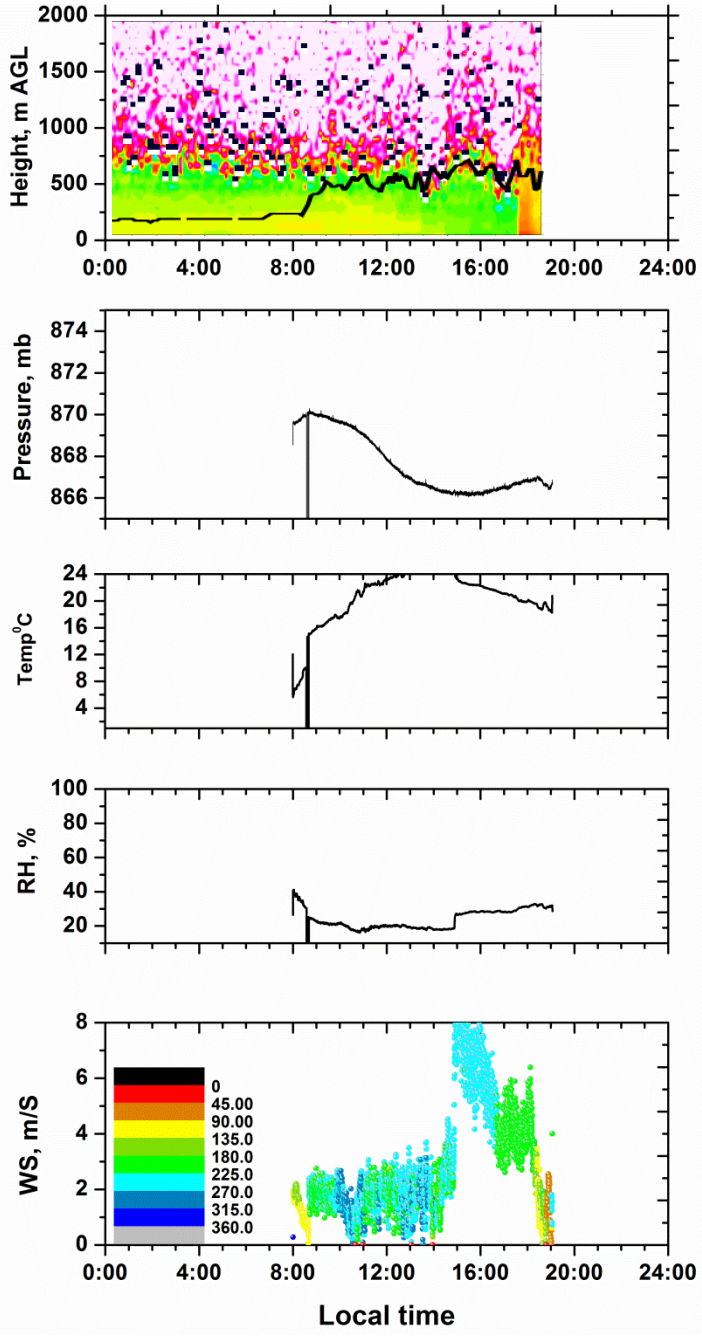

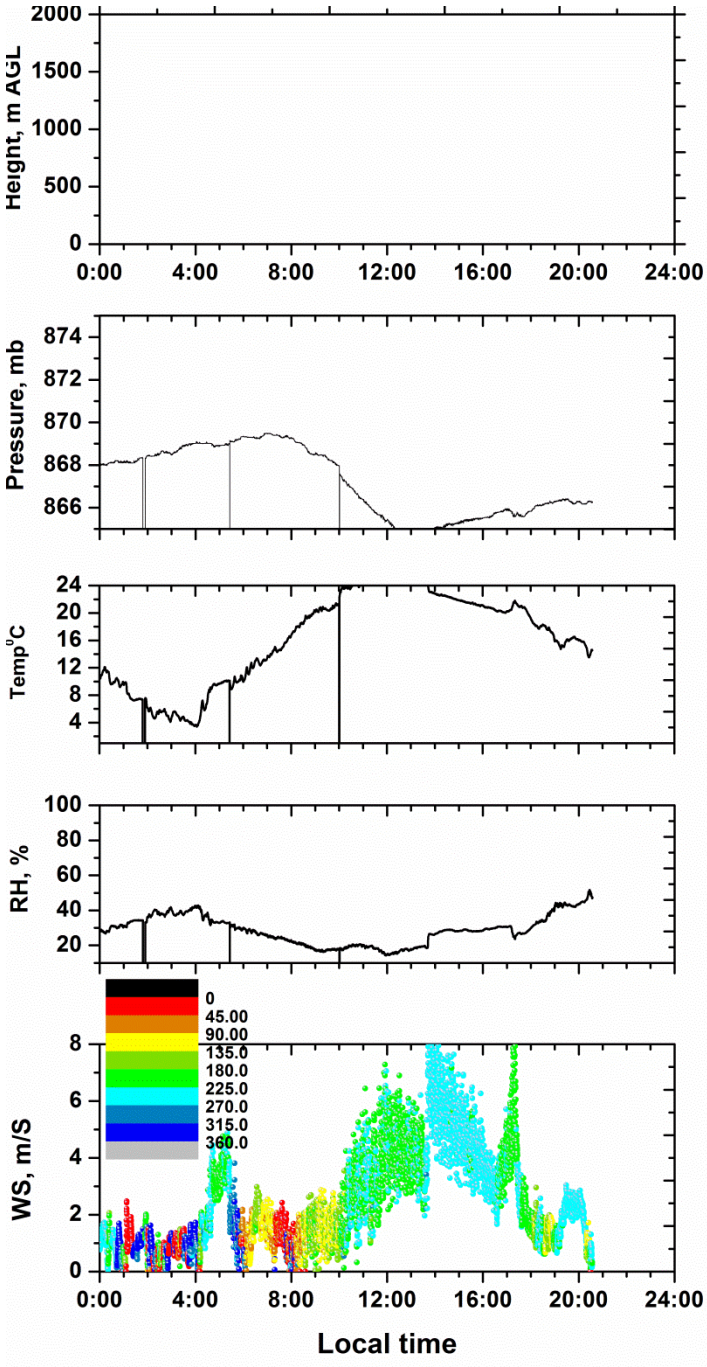

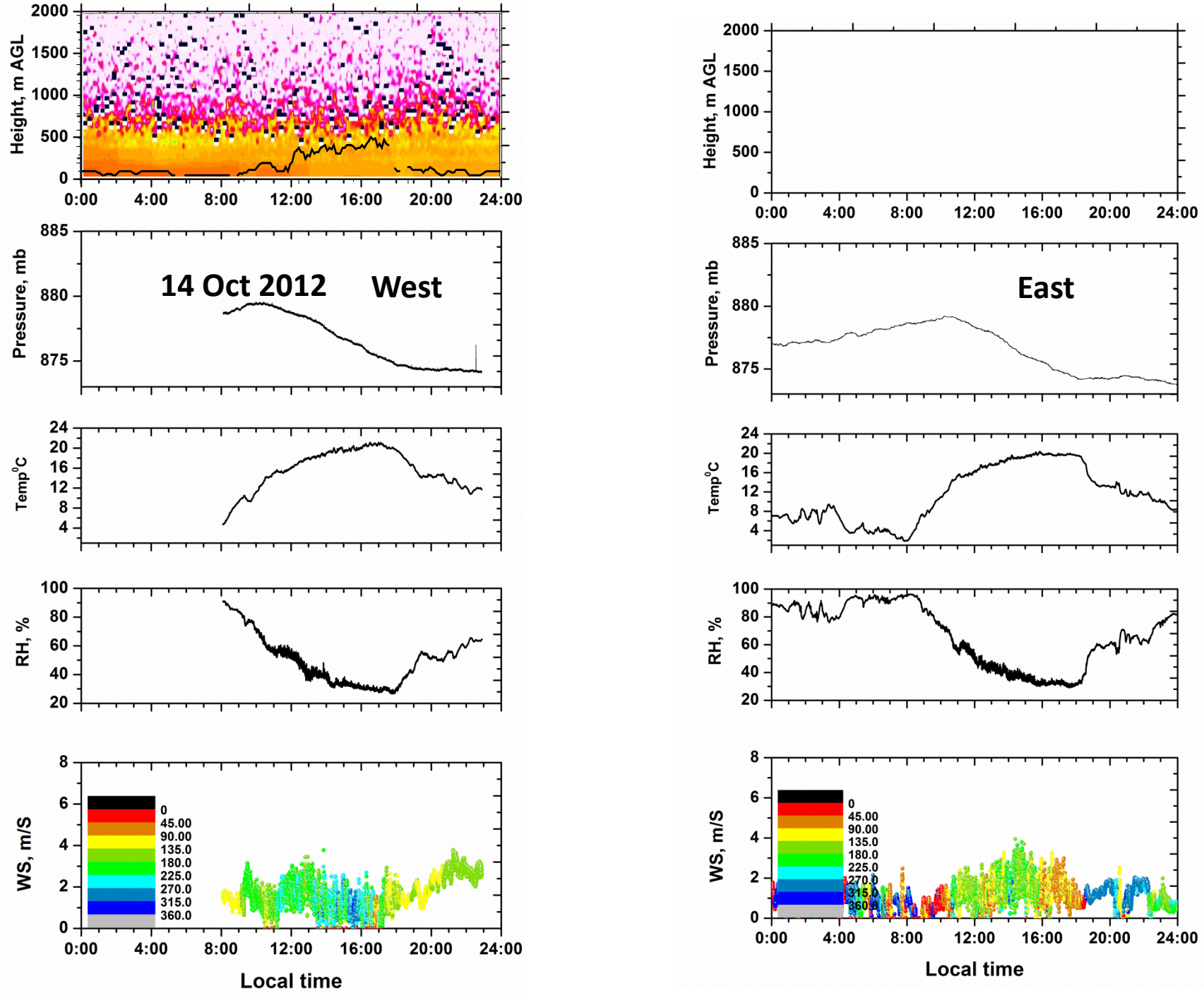
Height, m AGL
2000
1500
1000
500
0
0:00
4:00
8:00
12:00
16:00
20:00
24:00
Pressure, mb
885
880
875
14 Oct 2012
West
East
Temp^{0}C
24
20
16
12
8
4
RH, %
100
80
60
40
20
WS, m/S
6
4
2
0
0
45.00
90.00
135.0
180.0
225.0
270.0
315.0
360.0
Local time

15 Oct 2012

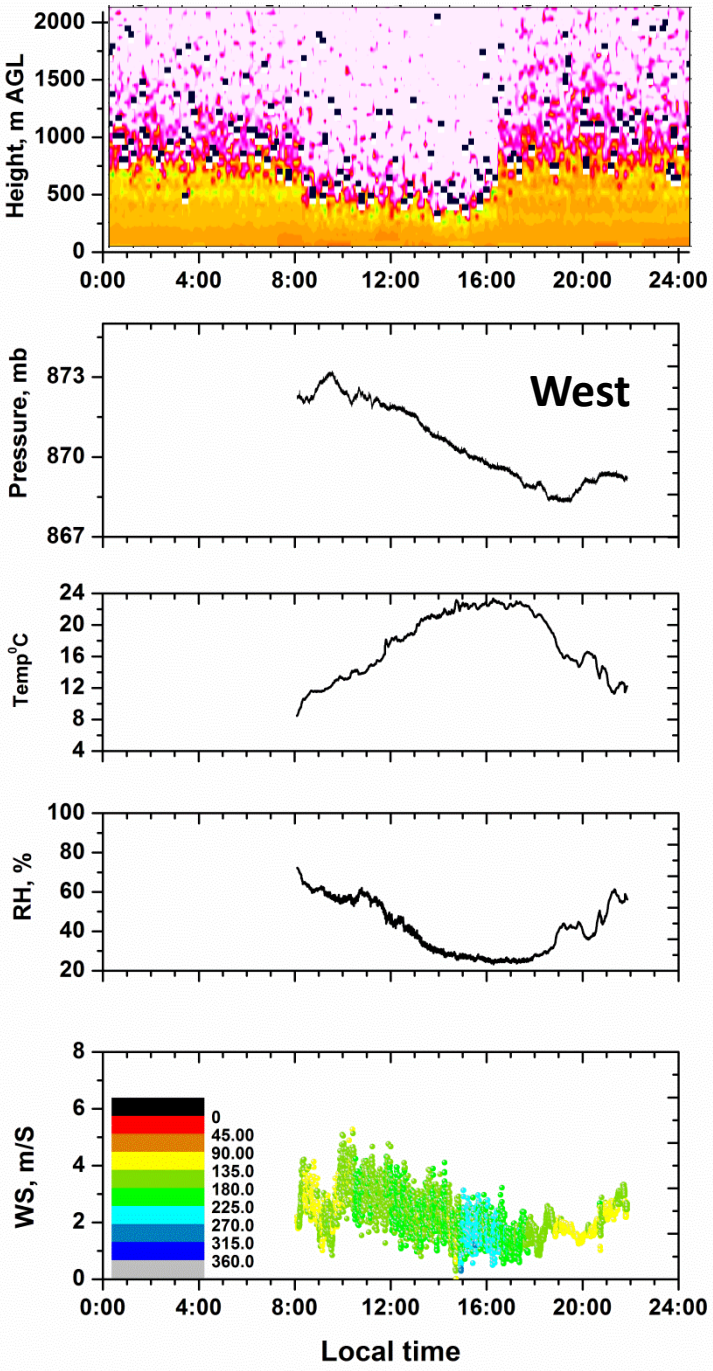
Height, m AGL
2000
1500
1000
500
0
0:00
4:00
8:00
12:00
16:00
20:00
24:00
Pressure, mb
873
870
867
West
Temp°C
24
20
16
12
8
4
RH, %
100
80
60
40
20
WS, m/S
8
6
4
2
0
0
45.00
90.00
135.0
180.0
225.0
270.0
315.0
360.0
Local time

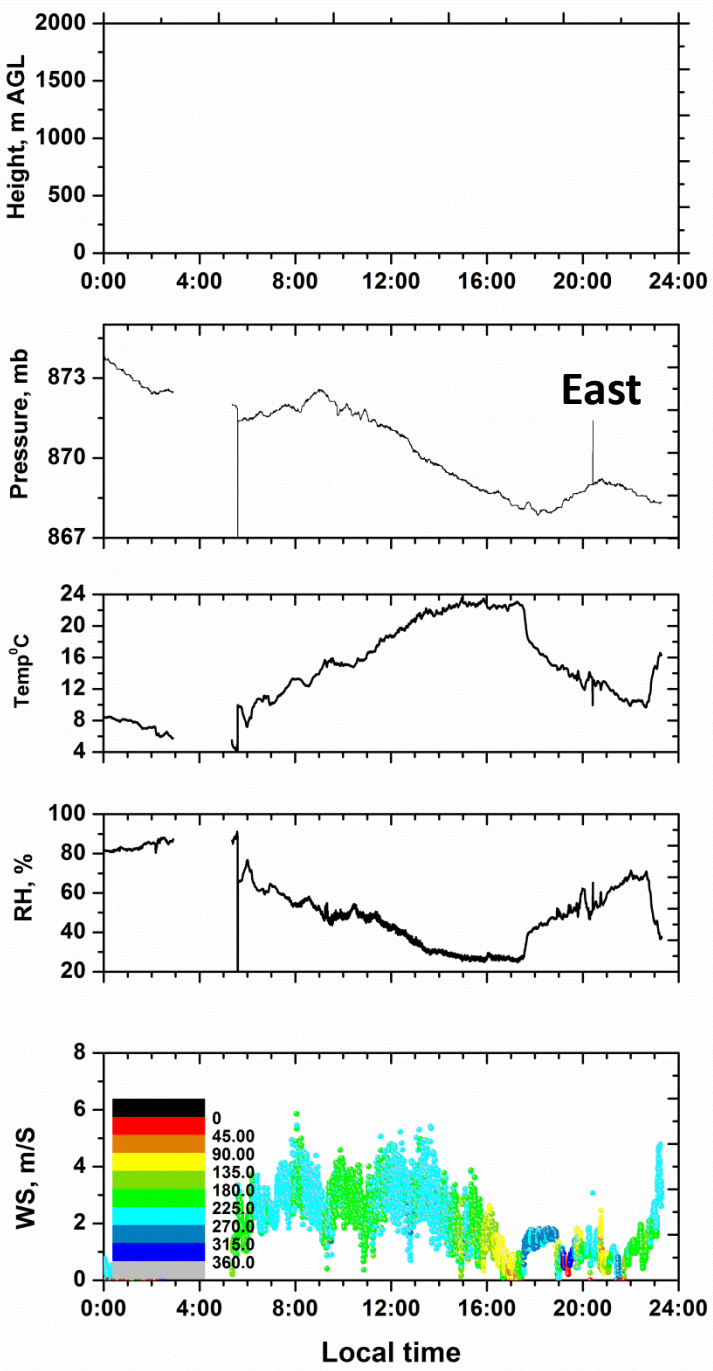
Height, m AGL
2000
1500
1000
500
0
0:00
4:00
8:00
12:00
16:00
20:00
24:00
Pressure, mb
873
870
867
East
Temp°C
24
20
16
12
8
4
RH, %
100
80
60
40
20
WS, m/S
8
6
4
2
0
0
45.00
90.00
135.0
180.0
225.0
270.0
315.0
360.0
Local time

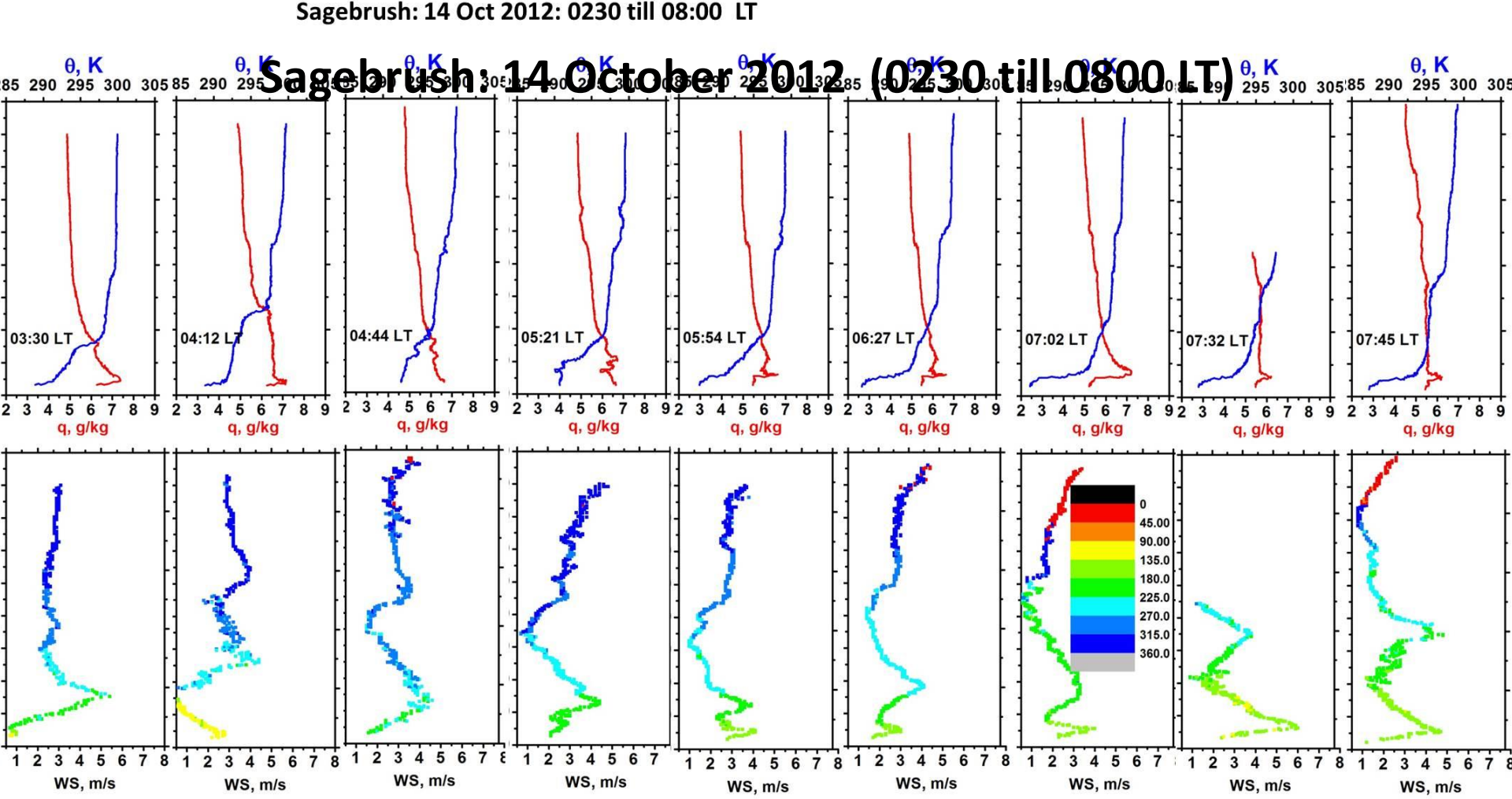

Application 01: NBL (often SBL) depths (Physical processes)

Application 02: Detection of the erosion of the NBL inversion (Physical processes)

Application 02a: Using 02 for ABL depth retrieval (Practical purpose: another candidate for attribution though for case studies)

Sagebrush: 14 October 2012 (0830 till 1330 LT)

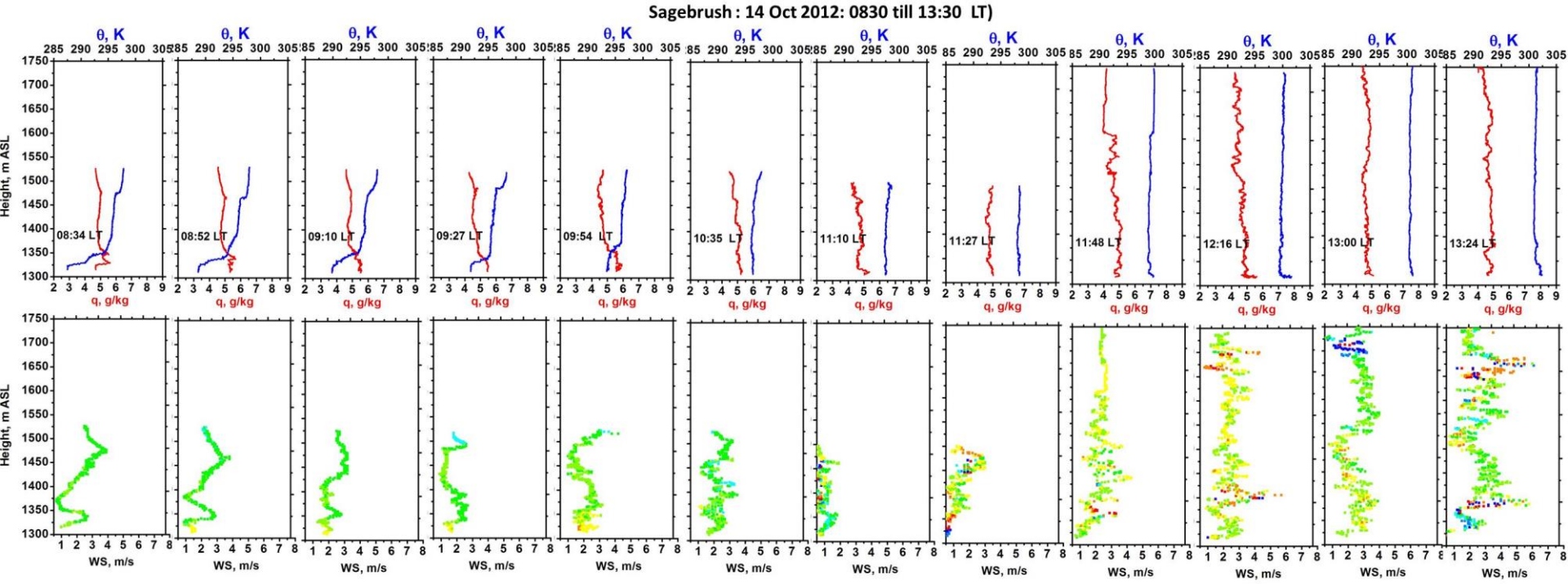

09-10 October IOP (Intercomparison)

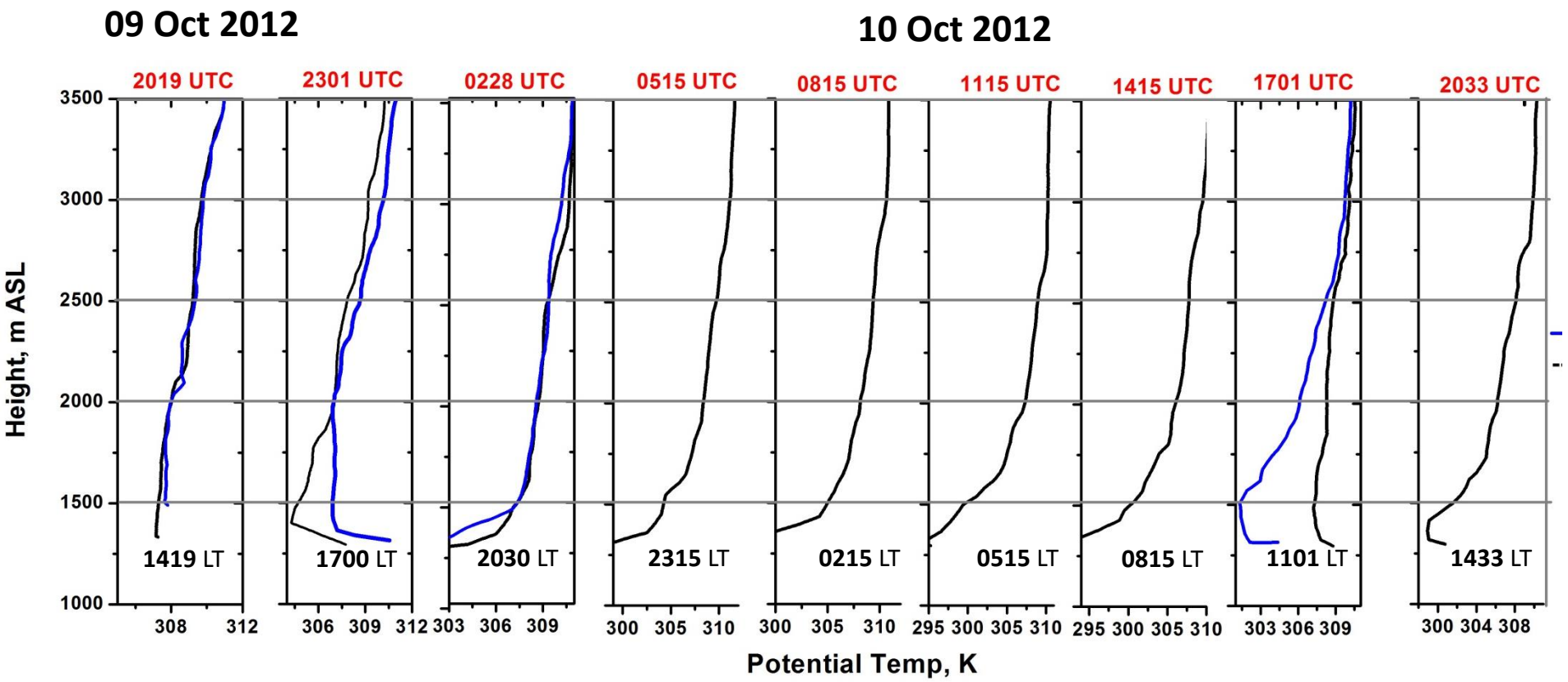

ABL depths determined with CL31 and RS: 09 October 2012

------- RS at Sagebrush

------- RS at Playa

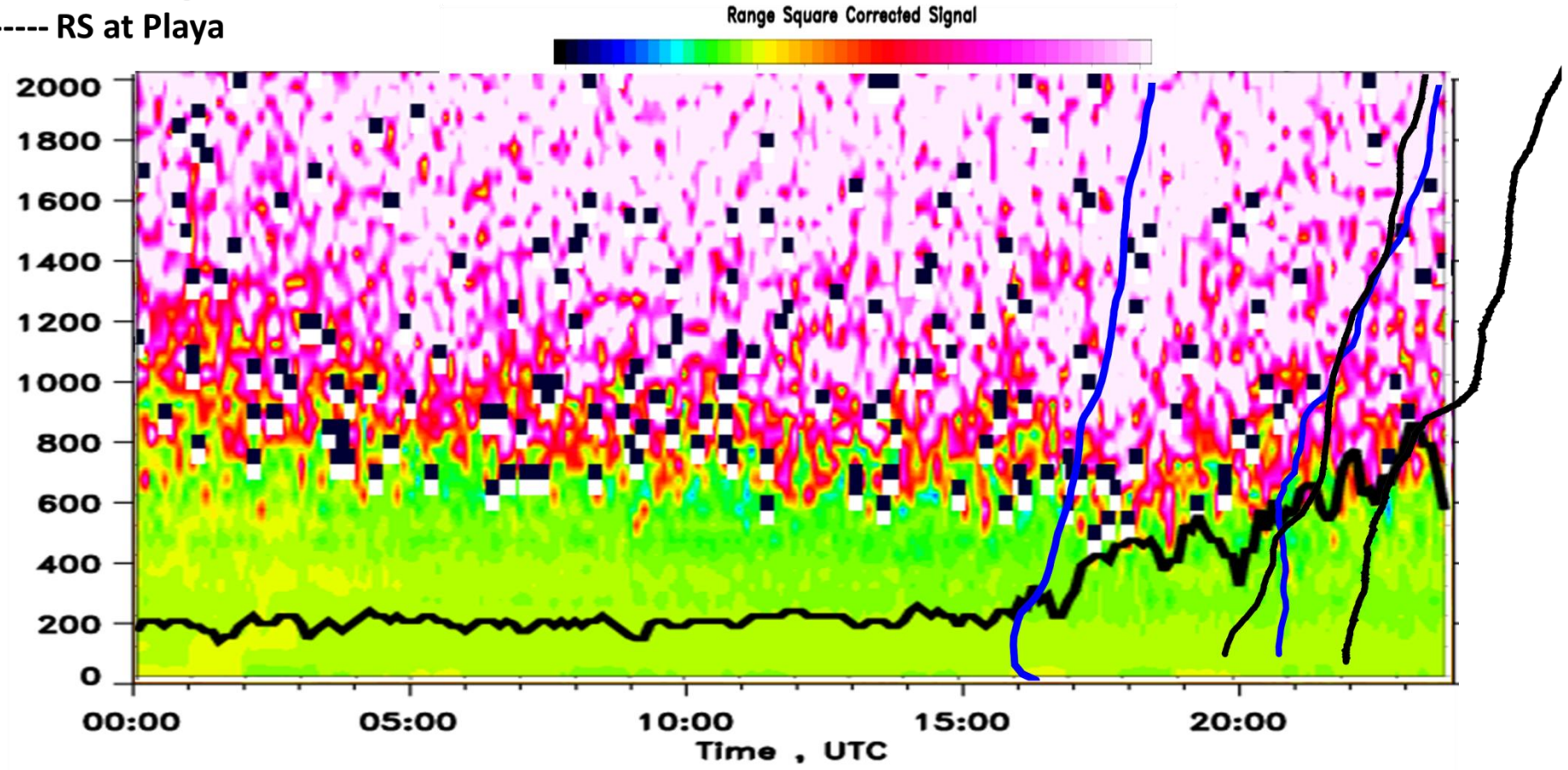

ABL depths determined with CL31 and RS: 10 October 2012

------- RS at Sagebrush

------- RS at Playa

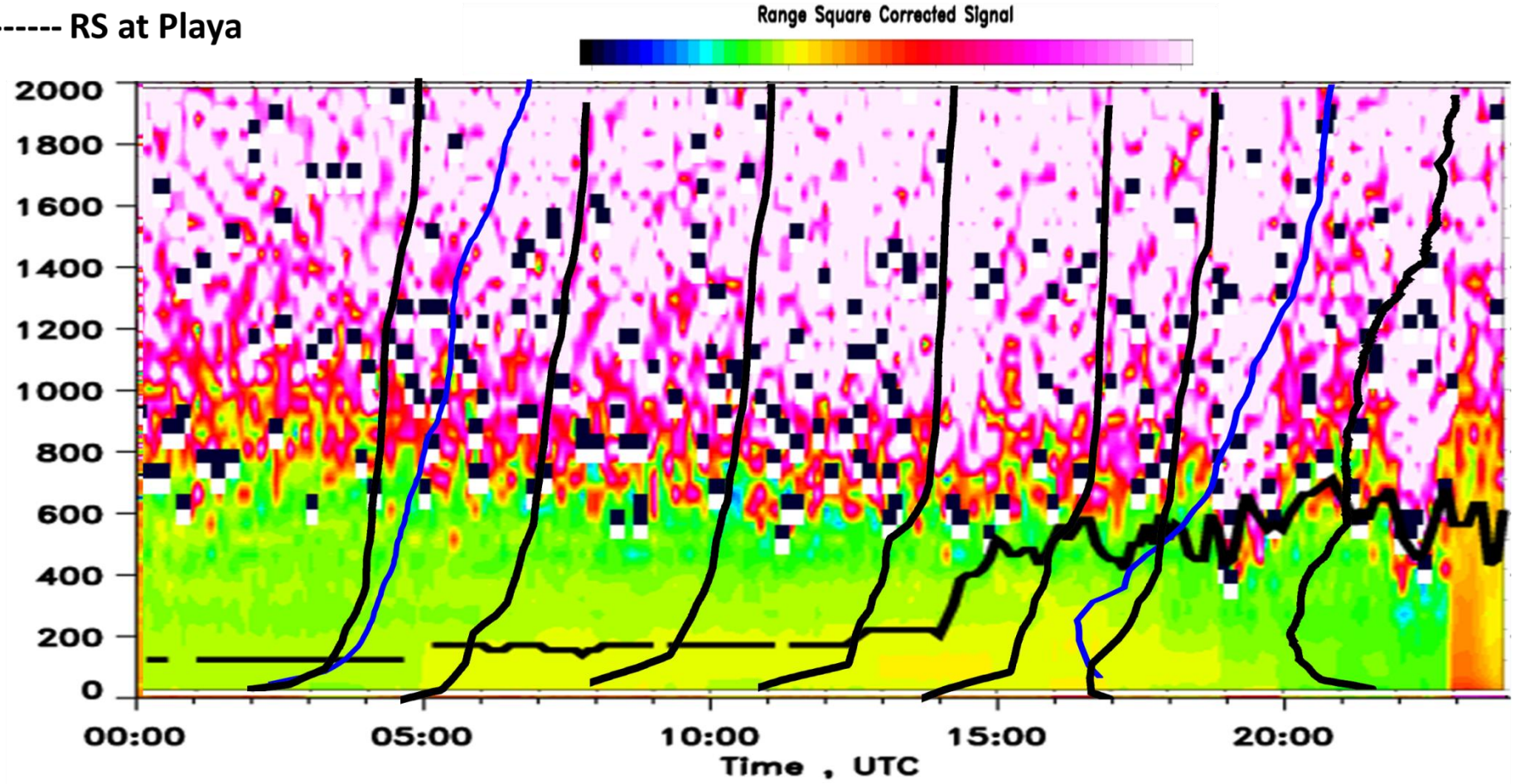

Radiosonde observation of thermodynamic variables: SB Site: 14 Oct

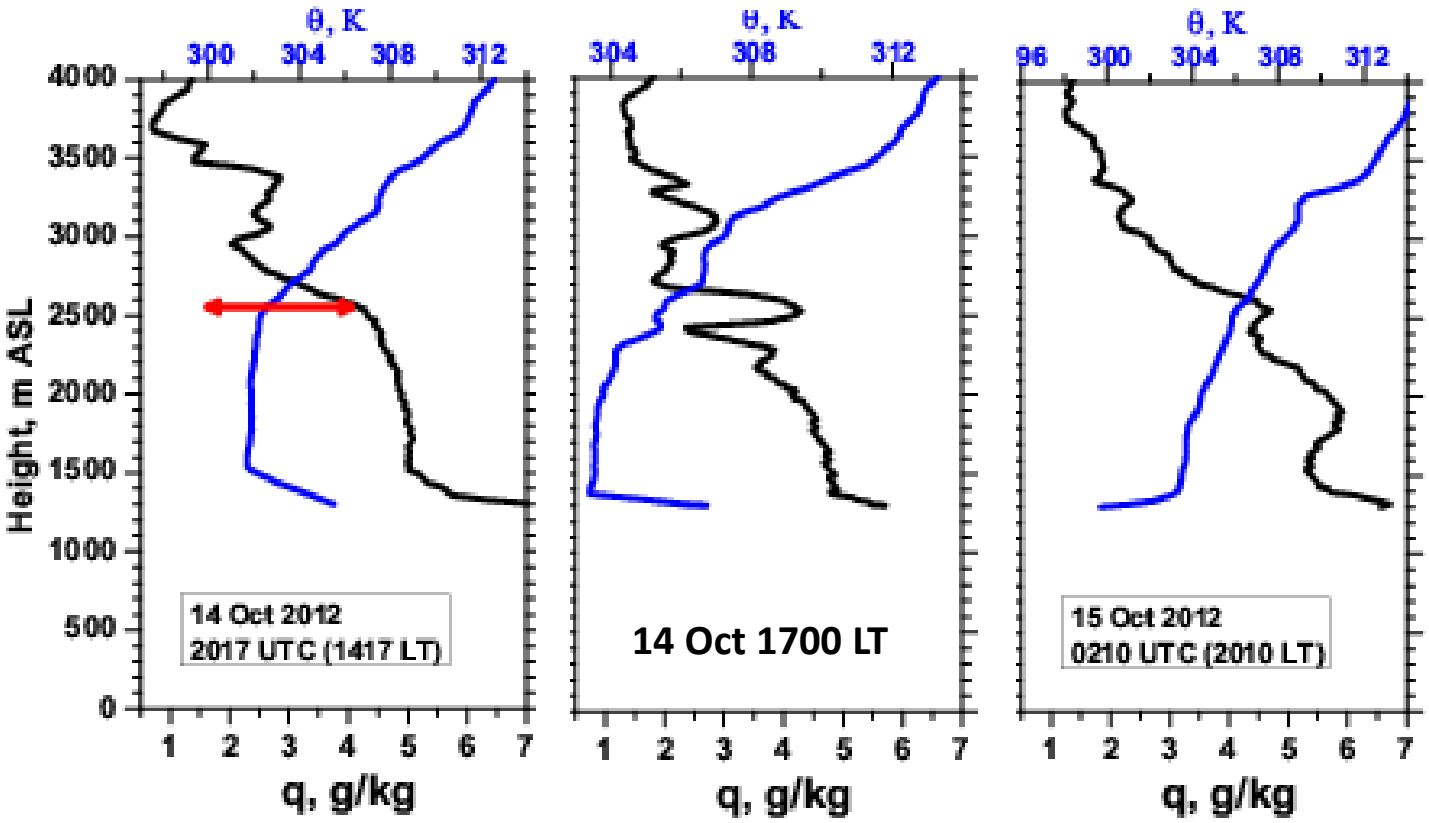

ABL depths
SB: 2600,2350, 200
Playa: 2300, 2200, 130

Frequency modulated continuous wave Radar
On 10 October

40.196902, -113.167763

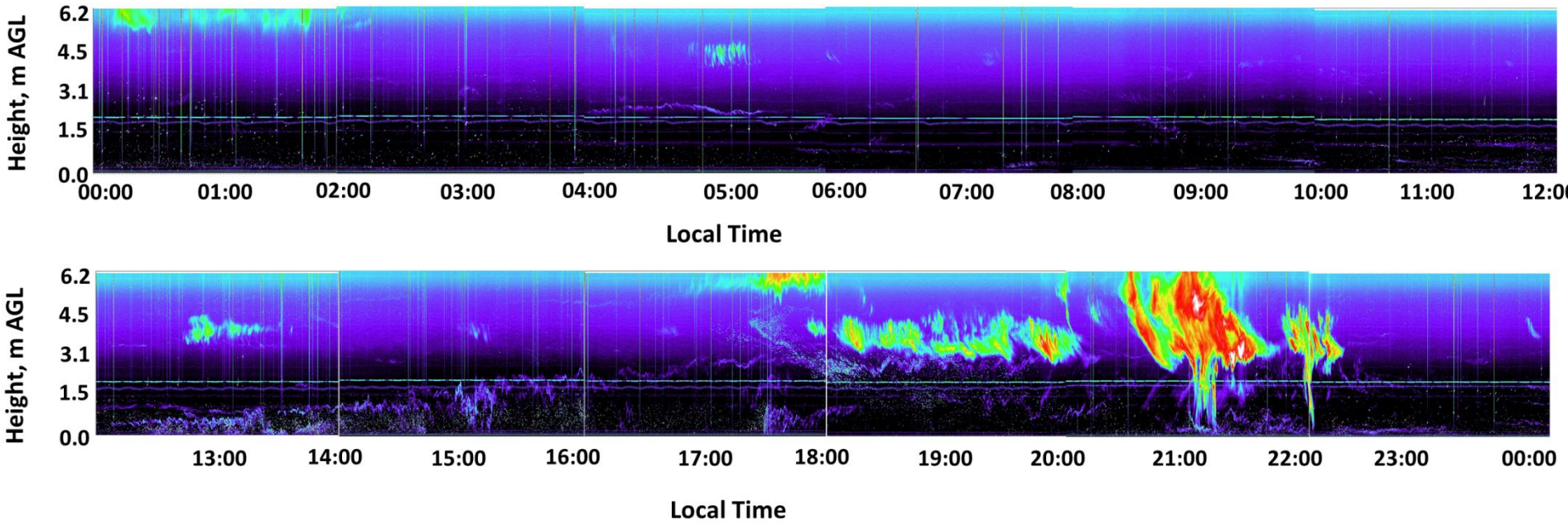

Further analyses on the spatial-variability of ABL depths

Davis, A., Marshak, A., Wiscombe, W., and Cahalan, R.: 1994, 'Multifractal characterizations of nonstationarity and intermittency in geophysical fields: Observed, retrieved, or simulated', J. Geophys. Res., 99, 8055-8072.

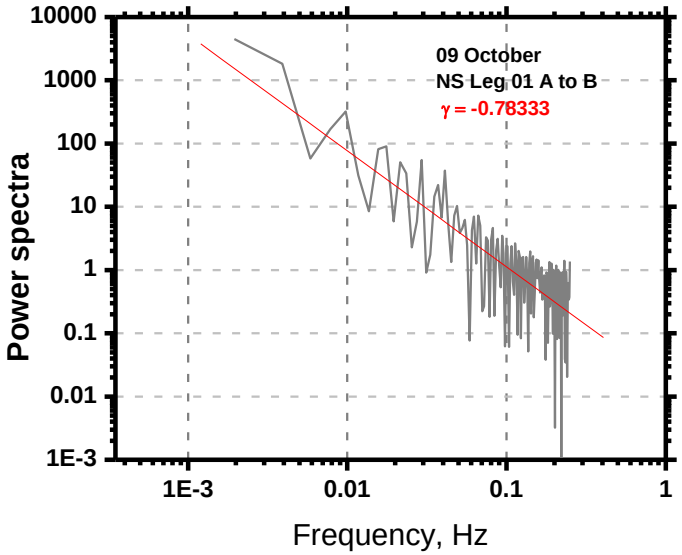

Multifractal characterizations of **nonstationarity** and **intermittency**...
onlinelibrary.wiley.com › ... › Vol 99 Issue D4
by A Davis - 1994 - Cited by 294 - Related articles
Sep 21, 2012 - **Multifractal characterizations** of **nonstationarity** and **intermittency** in **geophysical fields**: **Observed**, **retrieved**, or **simulated**. Anthony **Davis**; Alexander **Marshak**; Warren **Wiscombe**; Robert **Cahalan**. Article first published online: ... Volume **99**, Issue D4, pages **8055–8072**, 20 April **1994**. Additional Information ...

The power-law dependence can be found from $S_F(f) \sim f^{-\gamma}$ where S_F is the power and f is the frequency and γ is the corresponding spectral exponent. The slope of $\ln[S_F(f)]$ versus $\ln[f]$ yields the value of γ. The value of γ determines whether the process is self-affined or not. If $1 < \gamma < 3$ then, the signal is a non-stationary process with stationary increments.

Assisting lidar-estimated ABL depth measurements by ……..

Possible ways !!!

- Haar wavelet-based method (Subjective determination) (e.g., Pal et al., 2010 (ANGEO), Lac et al., 2013 (ACP))
- Combining ceilometer (for NBL) and lidar (CBL) time measurements (different limitations during different regimes, Behrendt et al., 2011 (QJRMS), Pal et al., 2012 (Atmos Env))
- Using surface-based turbulence measurements and combining gradient and variance profiles Pal et al., 2013 (JGR in review)
- **CO2 profiles and lidar measurements (in this presentation)**
- **Radon-tracer method (in the outlook of this talk)**
- **Assisting with near surface meteorological measurements, heat fluxes, other in-situ (Not explored so far, looking very much forward in the next days!!)**

Aerosol Stratification as well as ABL depths …